International Journal for Parasitology 39 (2009) 1289–1303

Contents lists available at ScienceDirect

International Journal for Parasitology

journal homepage: www.elsevier.com/locate/ijpara

6-Br-5methylindirubin-3′oxime (5-Me-6-BIO) targeting the leishmanial glycogen synthase kinase-3 (GSK-3) short form affects cell-cycle progression and induces apoptosis-like death: Exploitation of GSK-3 for treating leishmaniasis

Evangelia Xingi [a], Despina Smirlis [a], Vassilios Myrianthopoulos [b], Prokopios Magiatis [b], Karen M. Grant [c], Laurent Meijer [d], Emmanuel Mikros [b], Alexios-Leandros Skaltsounis [b], Ketty Soteriadou [a,*]

[a] Laboratory of Molecular Parasitology, Department of Microbiology, Hellenic Pasteur Institute, 127 Vas. Sofias Ave., 11521 Athens, Greece
[b] Laboratories of Pharmacognosy and Pharmaceutical Chemistry, Department of Pharmacy, University of Athens, Panepistimiopolis-Zografou, Athens 15771, Greece
[c] School of Health and Medicine, Lancaster University, LA1 4YB, UK
[d] C.N.R.S., Cell Cycle Group, Station Biologique, B.P. 74, 29682 Roscoff Cedex, Bretagne, France

ARTICLE INFO

Article history:
Received 11 February 2009
Received in revised form 31 March 2009
Accepted 3 April 2009

Keywords:
Leishmania donovani glycogen synthase kinase-3 short
5-Me-6-BIO
6-BIO
Indirubins
Apoptosis-like death
Drug target

ABSTRACT

Indirubins known to target mammalian cyclin-dependent kinases (CDKs) and glycogen synthase kinase (GSK-3) were tested for their antileishmanial activity. 6-Br-indirubin-3′-oxime (6-BIO), 6-Br-indirubin-3′acetoxime and 6-Br-5methylindirubin-3′oxime (5-Me-6-BIO) were the most potent inhibitors of *Leishmania donovani* promastigote and amastigote growth (half maximal inhibitory concentration (IC_{50}) values $\leqslant$1.2 μM). Since the 6-Br substitution on the indirubin backbone greatly enhances the selectivity for mammalian GSK-3 over CDKs, we identified the leishmanial GSK-3 homologues, a short (*Ld*GSK-3s) and a long one, focusing on *Ld*GSK-3s which is closer to human GSK-3β, for further studies. Kinase assays showed that 5-Me-6-BIO inhibited *Ld*GSK-3s more potently than CRK3 (the CDK1 homologue in *Leishmania*), whilst 6-BIO was more selective for CRK3. Promastigotes treated with 5-Me-6-BIO accumulated in the S and G2/M cell-cycle phases and underwent apoptosis-like death. Interestingly, these phenotypes were completely reversed in parasites over-expressing *Ld*GSK-3s. This finding strongly supports that *Ld*GSK-3s is: (i) the intracellular target of 5-Me-6-BIO, and (ii) involved in cell-cycle control and in pathways leading to apoptosis-like death. 6-BIO treatment induced a G2/M arrest, consistent with inhibition of CRK3 and apoptosis-like death. These effects were partially reversed in parasites over-expressing *Ld*GSK-3s suggesting that in vivo 6-BIO may also target *Ld*GSK-3s. Molecular docking of 5-Me-6-BIO in CRK3 and 6-BIO in human GSK-3β and *Ld*GSK-3s active sites predict the existence of functional/structural differences that are sufficient to explain the observed difference in their affinity. In conclusion, *Ld*GSK-3s is validated as a potential drug target in *Leishmania* and could be exploited for the development of selective indirubin-based leishmanicidals.

1. Introduction

Leishmaniasis is an umbrella term for a group of protozoan vector-borne parasitic diseases and manifests with three major forms, visceral, cutaneous and mucocutaneous. It is a significant cause of morbidity and mortality in developing countries, and affects about 2 million people per year mostly in tropical and sub-tropical regions (Alvar et al., 2006). Leishmaniasis is also an important public health and veterinary concern in Mediterranean countries (Dujardin, 2006). Chemotherapy for leishmaniasis is generally ineffective, mainly due to the emerging drug-resistance and severe toxic side effects (Croft et al., 2006). Antimonials are used as first-line treatment despite their toxicity. In case of antimonial resistance, liposomal formulations of amphotericin B, not devoid of adverse side effects, are used (Croft et al., 2006). Miltefosine, the first oral drug, has proved to be highly effective against visceral leishmaniasis. However, miltefosine-resistant parasites have been obtained in vitro indicating that there is a risk of resistance emerging in the field. Consequently there is an urgent need to discover new targeted drugs against leishmaniases (Croft et al., 2006).

Leishmania species are transmitted to mammals by the bite of a sand fly vector. During a sandfly blood meal, *Leishmania* promastigotes pass into the mammalian host where they penetrate macrophages and, within their phagolysosomes, transform into the non-flagellated, non-motile amastigote form and multiply (Chang, 1983). These trypanosomatid protozoan parasites have developed unusual and unique features in their cell biology to ensure adaptation to the contrasting environments of their insect and mammalian hosts that are reflected in the complexity of their cell- cycle

* Corresponding author. Tel.: +30 2106478841; fax: +30 2106423498.
E-mail address: ksoteriadou@pasteur.gr (K. Soteriadou).

0020-7519/$36.00 © 2009 Australian Society for Parasitology Inc. Published by Elsevier Ltd. All rights reserved.
doi:10.1016/j.ijpara.2009.04.005

control and during their differentiation. Therefore, differences between cell-cycle control in *Leishmania* and mammals may lead to the identification of essential molecules regulating the parasite cell-cycle that could be exploited for rational drug design (Naula et al., 2005). Potential parasite candidate targets include cyclin-dependent kinases (CDKs), glycogen synthase kinases (GSK-3), Aurora kinases and mitogen activated protein kinases (MAPKs) (Naula et al., 2005). Recently, it was shown that *Trypanosoma brucei* GSK-3 "short" is a potential drug target for trypanosomiasis therapy (Ojo et al., 2008). Efforts are therefore focused on the exploitation of kinase inhibitor libraries for the identification and further development of inhibitors that selectively target parasite kinases without damaging the host.

Indirubin analogues (collectively referred to as indirubins), a family of bis-indoles known for over a century as a minor constituent of plant, animal and microorganism-derived indigo, are powerful inhibitors of mammalian CDKs and GSK-3 by competing with ATP for binding to their catalytic site (Meijer et al., 2003; Polychronopoulos et al., 2004). 6-Bromo substituted indirubins display higher selectivity for mammalian GSK-3 over CDKs (Meijer et al., 2003; Polychronopoulos et al., 2004). In cell-based assays, indirubins display anti-mitotic and anti-tumoral activity and induce arrest in G1 or G2/M phase of the cell-cycle, depending on the cell line (Hoessel et al., 1999; Damiens et al., 2001). Specifically, 6-bromo-indirubin-3′-oxime (6-BIO) induces apoptotic death in neuroblastoma cells (Ribas et al., 2006).

GSK-3 is a multifunctional serine/threonine kinase found in all eukaryotes. This enzyme is known to play a key role in many cellular and physiological events, including Wnt signalling, transcription, cell-cycle and differentiation, neuronal functions and circadian rhythm (Frame et al., 2001; Doble and Woodgett, 2003). These functions of GSK-3 and its implication in many human diseases such as Alzheimer's disease, non-insulin-dependent diabetes mellitus and cancer have stimulated an active search for potent and selective GSK-3 inhibitors, such as indirubins (Meijer et al., 2004).

CRK3, a leishmanial CDK1 homologue, displaying 54% identity and 71% similarity with human CDK1, has been validated as a drug target (Grant et al., 1998; Hassan et al., 2001). Three indirubins (5-sulphonamide-indirubin-3′oxime, 5-SO_3Na-3′oxime and 5-SO_3H) have been shown to inhibit CRK3 with IC_{50} values of 11, 16 and 47 nM, respectively, and *Leishmania donovani* infection of mouse macrophages with half maximal inhibitory concentration (IC_{50}) values of 3.56, 5.8 and 7.6 μM, respectively (Grant et al., 2004; Wells et al., 2006). *Leishmania mexicana* promastigotes treated with indirubins displayed growth arrest and disruption of cell-cycle, in line with the inhibition of a CDK (Grant et al., 2004).

In this study, 16 indirubins were tested for their antileishmanial activity and three, 6-BIO, 6-BIA and 5-Me-6-BIO, were found to be the most powerful inhibitors of both *L. donovani* promastigotes and intracellular amastigote growth. Since the 6-Br substitution on the indirubin backbone greatly enhances the selectivity for mammalian GSK-3 over CDKs, we identified the leishmanial GSK-3 homologues, a short (*Ld*GSK-3s) and a long one (*Ld*GSK-3l). We then investigated whether our compounds target *Ld*GSK-3s which is closer to human GSK-3β. *Ld*GSK-3s was identified as the predominant intracellular target of 5-Me-6-BIO. Evidence is also presented that *Ld*GSK-3s is involved in cell-cycle control as well as in pathways leading to apoptosis-like death.

2. Materials and methods

2.1. Cell culture

Leishmania donovani (strain LG13, MHOM/ET/0000/HUSSEN) promastigotes and the murine macrophage J774 cell line (ATCC) were cultured in medium 199 (M199) and RPMI 1640 (RPMI), respectively, both supplemented with 10% heat inactivated FBS (HI-FBS), 10 mM Hepes and antibiotics. Axenic *L. donovani* amastigotes were generated as previously described (Barak et al., 2005; Smirlis et al., 2006). Spleen-derived *L. donovani* amastigotes were maintained in Schneider's insect medium pH 5.5 supplemented with 20% HI-FBS at 37 °C. *Leishmania donovani* transfectants with the *Leishmania* expression vector pLEXSY-sat, the *L. donovani* glycogen synthase kinase-3 short cloned in pLEXSY-sat (pLEXSY-sat-*Ld*GSK-3s) and the *Ld*GSK-3s kinase-dead mutant cloned in pLEXSY-sat (pLEXSY-sat-*Ld*GSK-3s/K49R) were cultured in M199 supplemented with 100 μg/ml nourseothricin (Jena Bioscience). *Leishmania mexicana* CRK3his transfectants were cultured as described previously (Grant et al., 2004).

2.2. Chemical library

The chemical library consists of 16 indirubins (Table 1), synthesised as previously described, (Polychronopoulos et al., 2004; Ribas et al., 2006). The compounds were dissolved in DMSO at 10 mM and serial dilutions in DMSO were made (1 mM and 100 μM). Indirubins were diluted in culture medium to give the desired final concentrations.

2.3. In vitro testing of the antileishmanial activity of indirubins against *L. donovani* promastigotes, intracellular amastigotes and axenic amastigotes

The Alamar blue assay (Mikus and Steverding, 2000) was applied for determining the antileishmanial activity of indirubins and Amphotericin B (Fungizone) was used as a reference drug. Stationary-phase *L. donovani* promastigotes (2×10^7 cells/ml) were seeded into 96-well flat bottom plates at a density of 2.5×10^6 cells/ml in 200 μl M199 without phenol red, containing increasing indirubin concentrations or the equivalent volume of the diluent DMSO, each in quadruplicate. The final concentration of DMSO was always <1% (v/v) and did not affect the growth of parasites. Following indirubin treatment for 72 h, Alamar blue (20 μl/well) was added and the plates were incubated at 26 °C for a further 12 h. Colorimetric readings were performed at a test wavelength of 550 nm and a reference wavelength of 620 nm. Comparison of DMSO-treated controls with samples allowed the calculation of the concentration of indirubin necessary to reduce the growth rate of promastigotes by 50% (IC_{50} values).

To evaluate the inhibitory activity of indirubins on intracellular amastigotes we treated infected macrophages for 72 h with indirubins and then assessed amastigote survival by lysing infected macrophages using the Alamar blue assay. Briefly, J774 macrophages (2×10^5 cells/ml in 200 μl RPMI) were left to adhere overnight at 37 °C in 5% CO_2 into 96-well flat bottom plates. Macrophages were infected with stationary-phase *L. donovani* promastigotes at a ratio of 10 parasites/macrophage and incubated for a further 24 h at 37 °C in 5% CO_2 as previously described (Papageorgiou and Soteriadou, 2002). Then the overlying medium was removed and cells were washed three times in fresh RPMI. Fresh RPMI was added containing increasing concentrations of indirubins or the equivalent volume of the diluent DMSO, each in quadruplicate. After 72 h, the medium was removed and infected cells were lysed by addition of 100 μl 0.01% SDS in PBS for 30 min at 37 °C. Then 100 μl Schneider's medium was added to each well that contained the liberated amastigotes (Papageorgiou and Soteriadou, 2002). Amastigote growth was assessed by the addition of Alamar blue (20 μl/well) and the plates were incubated for 48 h at 37 °C. Comparison of DMSO-treated controls with samples enabled the calculation of the degree to which infection had been inhibited by the presence of indirubins and to calculate the concentration that reduces the number of amastigotes by 50%.

Table 1
Indirubin compounds tested in vitro for their antileishmanial activity against *Leishmania donovani* promastigotes (P), intracellular amastigotes (In. A) and axenic amastigotes (Ax. A) using the Alamar blue assay.

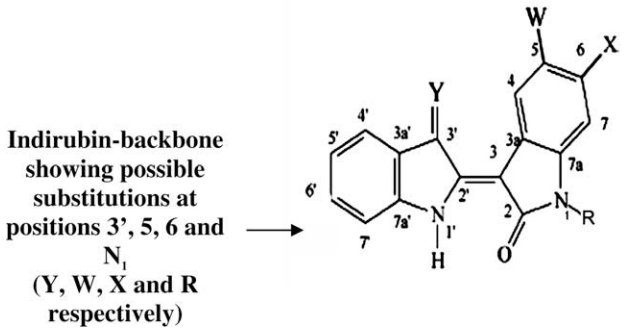

Compound	Y	X	W	R	*L. donovani* IC_{50}* (μM)		
					P	In. A	Ax. A
Indirubin	O	H	H	H	n.i.[a]	n.i.	n.i.
Indirubin-3′oxime	NOH	H	H	H	n.i.	n.i.	n.i.
5-Br-indirubin	O	H	Br	H	n.i.	n.i.	n.i.
5-Br-indirubin-3′oxime (5-BIO)	NOH	H	Br	H	5.2 ± 1.6	1 ± 0.15	1 ± 0.2
5-Aminoindirubin-3′oxime	NOH	H	NH_2	H	>10 [b]	>10	>10
6-Br-indirubin	O	Br	H	H	n.i.	n.i.	n.i.
6-Br-indirubin-3′oxime (6-BIO)	NOH	Br	H	H	0.8 ± 0.1	0.75 ± 0.05	0.9 ± 0.1
6-Br-*N*-methyl-indirubin-3′-oxime	NOH	Br	H	CH_3	n.i.	n.i.	n.i.
6-Br-indirubin-3′acetoxime (6-BIA)	NOAc	Br	H	H	0.9 ± 0.1	1 ± 0.05	1 ± 0.1
6-Br-*N*-methyl-indirubin-3′acetoxime	NOAc	Br	H	CH_3	n.i.	n.i.	n.i.
6-Br-indirubin-3′diethyl phosphatoxime	$NOPO(OEt)_2$	Br	H	H	>10	>10	>10
Indirubin-3′-methoxime	$NOCH_3$	H	H	H	n.i.	n.i.	n.i.
6-Br-5nitroindirubin	O	Br	NO_2	H	n.i.	n.i.	n.i.
6-Br-5nitroindirubin-3′-oxime	NOH	Br	NO_2	H	>10	>10	>10
6-Br-5methylindirubin	O	Br	CH_3	H	n.i.	n.i.	n.i.
6-Br-5methylindirubin-3′oxime (5-Me-6-BIO)	NOH	Br	CH_3	H	1.2 ± 0.2	1 ± 0.1	1 ± 0.2

* IC_{50} values were determined from dose–response curves and are expressed in μM.
[a] n.i., no inhibition at 50 μM.
[b] IC_{50} values ranging between 10 and 50 μM.

Leishmania donovani axenic amastigotes were treated with the inhibitors and the percentages of growth inhibition were assessed by addition of Alamar blue after 72 h of treatment (Habtemariam, 2003). In all cases, IC_{50} values were determined from dose–response curves via linear interpolation.

2.4. Analysis of indirubin-treated promastigotes by flow cytometry

Stationary-phase (2×10^7 cells/ml) *L. donovani* promastigotes were seeded at 10^6 cells/ml in M199 and incubated at 26 °C in the presence of DMSO (the diluent, used as control) or the tested indirubin. Preparation of samples for fluorescence-activated cell sorting (FACS) analysis of the cell-cycle was carried out as described by Smirlis et al. (Smirlis et al., 2006). Exposed phosphatidylserine on the outer membrane of cells and plasma membrane integrity of cells were assessed using Annexin V-FITC and propidium iodide (PI) staining (Apoptosis Detection kit, R&D Systems). Preparation of samples for FACS analysis was performed according to the manufacturer's instructions. In all cases, 20,000 cells/sample were analysed, using a Becton Dickinson FACSCalibur flow cytometer and data were analysed using the Cell Quest software. All experiments were performed at least three times.

2.5. Cellular and nuclear morphology

Stationary-phase *L. donovani* promastigotes were seeded at 10^6 cells/ml and incubated with either 2 μM indirubin or DMSO for 24 and 48 h. Cells were fixed in 2% paraformaldehyde and treated with 50 μg/ml RNaseA and 10 μg/ml PI. Parasites were observed under a TCSSP Leica Confocal fluorescence microscope. At least 100 cells from three independent experiments were recorded for each condition.

2.6. Cell count and viability assay

Stationary-phase *L. donovani* promastigotes were seeded at 10^6 cells/ml and incubated with either 2 μM 5-Me-6-BIO or DMSO for 24, 48 and 72 h. Cells were then washed twice in PBS, resuspended in drug-free medium and allowed to recover for 24, 48 and 72 h. The viability assay at different time points after exposure of parasites to 5-Me-6-BIO and drug removal was assessed using 0.4% Trypan blue solution. Both total cell count and the percentages of viable and non-viable cells were recorded. The experiment was performed three times.

2.7. In situ labelling of DNA fragments by TUNEL

In situ detection of DNA strand breaks was performed using the Cell Death Fluorescein Detection kit (Roche Applied Science) following the manufacturer's instructions. Samples were analysed under a Zeiss fluorescence microscope at 120× magnification. The ratio of apoptosis (apoptotic to total cells) was determined by counting at least 400 cells per group in three independent experiments.

2.8. Gene cloning and antibody production

The *L. donovani GSK-3s* gene was amplified by PCR from *L. donovani* (strain LG13, MHOM/ET/0000/HUSSEN) genomic DNA, using a sense primer 5′-ACC GCC ATG GAC ATG TCG CTC AAC GCT GC-3′

and an antisense primer 5′-CCC CCT CGA GCT GCT TGC GAA CTA GCT T-3′, that were designed based on the gene coding for the shorter of the two *Leishmania major Friedlin* GSK-3 proteins (LmjF18.0270). The amplified PCR product was cloned into the NcoI-XhoI site of pTriEx-1.1 vector (Novagen), a construct allowing the addition of a poly-Histidine extention to the C-terminus of the recombinant protein (pTriEx-1.1-*Ld*GSK-3s). The cloned gene was then sequenced and compared with the short sequence of *Leishmania infantum* GSK-3 (LinJ18_V3.0270). The *Ld*GSK-3s DNA and protein sequences were found to be identical to the *L. infantum* GSK-3s sequences. *Ld*GSK-3s nucleotide sequence was deposited in GenBank (EF620873). The pTriEx-1.1-*Ld*GSK-3s construct was transformed into bacteria and $(His)_6$-tagged *Ld*GSK-3 was purified by Metal-Affinity Chromatography (Qiagen Ni–NTA Superflow resin). *Ld*GSK-3s was detected using a polyclonal IgG His-probe antibody (1:500 dilution, stock solution 200 μg/ml, Santa Cruz Biotechnology) and a polyclonal anti-ratGSK-3β antibody. The recombinant protein was subsequently used to immunize a New Zealand white rabbit using the scheme described in a previous study (Smirlis et al., 2006). The immunization protocols were approved by the Ethical Committee of Hellenic Pasteur Institute and were in accordance with the European Directive 86/609/EEC on the protection of animals used in research. Affinity purified anti-*Ld*GSK-3s antibody was isolated by low pH elution of antibodies bound to purified *Ld*GSK-3s on nitrocellulose strips, as previously described (Smirlis et al., 2006).

2.9. Generation of transgenic promastigotes and purification of LdGSK-3s and CRK3

The DNA encoding $(His)_6$-tagged *Ld*GSK-3s was amplified by PCR from the construct pTriEx-1.1-*Ld*GSK-3s, described above. Sense and antisense primers for the amplification were 5′-ACC GCC ATG GAC ATG TCG CTC AAC GCT GC-3′ and 5′-GCA GGC GGC CGC TGA GGT TAA TCA CTT AGT G-3′, respectively. The PCR product was then cloned in the NcoI and NotI sites of the *Leishmania* expression vector pLEXSY-sat (pF4X1.4sat) (Jena Bioscience) to generate the pLEXSY-sat-*Ld*GSK-3s plasmid. The cloned gene was sequenced to confirm the correct orientation. Site-directed mutagenesis was performed on *Ld*GSK-3s in pLEXSY-sat-*Ld*GSK-3s construct, using the Phusion® Site-Directed Mutagenesis Kit (Finnzymes) following the manufacturer's protocol. Primers used for Lysine 49 to Arginine mutation (K49R) were as follows: Forward 5′-GAGCGTGGCGATCCGGAAGGTTATCCAGGAC-3′ and Reverse 5′-ATGCCCGTCGACTTCTCCTTGCCTAGTTGCA-3′. The K49R mutation in the construct pLEXSY-sat-*Ld*GSK-3s/K49R was confirmed by sequencing.

Leishmania donovani transfectants with pLEXSY-sat, pLEXSY-sat-*Ld*GSK-3s and pLEXSY-sat-*Ld*GSK-3s/K49R plasmids (supercoiled, transfected as episomes) were generated as previously described (Smirlis et al., 2006). Selection of transgenic promastigotes was performed in M199 containing 100 μg/ml nourseothricin.

Purification of *Ld*GSK-3s from *L. donovani* sat-*Ld*GSK-3s transfectants and of *Ld*GSK-3s/K49R from sat-*Ld*GSK-3s/K49R transfectants as well as of CRK3 from transgenic *L. mexicana* promastigotes was carried out as previously described (Grant et al., 2004). *Ld*GSK-3s and CRK3 were stored with 10% glycerol at −80 °C for kinase assays.

2.10. Immunoblotting

Parasites were suspended in lysis buffer (50 mM 3-(N-morpholino)propanesulfonic acid (MOPs) pH 7.5, 100 mM NaCl, 1 mM EDTA, 1 mM EGTA, 1 mM Na_3VO_4, 10 mM NaF, 1% Triton X-100) supplemented with protease inhibitors (0.1 mg/ml leupeptin, 1 mM phenylmethanesulphonylfluoride (PMSF), 5 μg/ml aprotinin, 5 μg/ml pepstatin A, 1 mM phenanthroline) and Laemmli sample buffer was added. Whole cell lysates were resolved by 12% SDS–PAGE, transferred to nitrocellulose membranes and subsequently probed with the appropriate primary antibodies: a polyclonal anti-ratGSK-3β antibody [directed against the C-terminal sequence CAHSFFDELRDPNVK, residues identical between rat and *Ld*GSK-3s are underlined] (1:100 dilution, stock solution 500 μg/ml, Abcam); the generated anti-*Ld*GSK-3s rabbit polyclonal antibody (1:1000 dilution) and the polyclonal IgG His-probe antibody (1:200 dilution). After incubation with peroxidase-conjugated secondary antibody, 3,3′-diaminobenzidine was used for detection.

To demonstrate equal loading of cells, the blot was stripped and re-probed with antiserum against *L. infantum* myo-inositol-1-phosphate synthase (LinJ14_V3.1450, INO1), reported to be equally expressed in *L. mexicana* promastigotes and amastigotes (Ilg, 2002). The *INO1* gene was PCR-amplified from *L. infantum* genomic DNA, using a sense primer 5′-CAAGGGATCCGATGACGCGTGACATG GACG-3′ and an antisense primer 5′-GGCACTC GAGCAGCATGTT GCTGTCGG-3′, cloned into the BamHI and XhoI site of pTriEx-1.1, in frame with a C terminal his-tag, expressed in *Escherichia coli* and purified on Ni^{+2}- nitrilotriacetate (Ni–NTA) resin. Anti-*Lin* INO1 antibody was produced and purified, using nitrocellulose strips with purified INO1, as previously described (Smirlis et al., 2006).

2.11. Immunofluorescence

Parasites were fixed in 2% formaldehyde and 0.05% glutaraldehyde. Cells were blocked in 50 mM NH_4Cl containing 3% BSA in PBS and treated with 50 μg/ml RNaseA. Nuclei were stained with 10 μg/ml PI followed by incubation for 5 h with either anti-*Ld*GSK-3s or the anti-ratGSK-3β antibodies (10 or 5 μg/ml, respectively) in PBS containing 0.1% Triton X-100 and 3% BSA. The bound antibody was detected with 1:100 diluted FITC conjugated anti-rabbit or anti-rat IgG antibody (Sigma). Cells were observed with a TCSSP Leica Confocal fluorescence microscope.

2.12. Kinase assays

Kinase assays were performed with purified *Ld*GSK-3s and CRK3 from *L. donovani* over-expressing transfectants and transgenic *L. mexicana* promastigotes, respectively (Supplementary Fig. S1). The kinase activity of *Ld*GSK-3s was assayed using GS-1 peptide (YRRAAVPPSPSLSRHSSPHQSpEDEEE) as a substrate; GS-1 peptide was patterned after the GSK-3 phosphorylation sites of mammalian glycogen synthase (Meijer et al., 2004). CRK3 kinase assays were performed using histone H1 substrate as previously described (Grant et al., 2004). All assays were performed in the kinase assay buffer (50 mM MOPS pH 7.2, 20 mM $MgCl_2$, 10 mM EGTA, 2 mM DTT) in the presence of [γ-^{33}] ATP (3000 Ci/mmol; 1 mCi/ml) in a final volume of 30 μl and incubated for 30 min at 30 °C as previously described (Meijer et al., 2004). Initially the K_m values for ATP and substrate for each kinase were measured. The K_m values for ATP for both kinases were around 15 μM (15.2 μM for *Ld*GSK-3s and 14.78 μM for CRK3). In order to determine the IC_{50} values with the inhibitors, we used ATP and substrate concentrations at the calculated K_m values. For both *Ld*GSK-3s and CRK3 15 μM ATP were used in the assays, in the presence of 8.3 μM GS-1 peptide and 5 μM histone H1, respectively. K_i values for each inhibitor were calculated using the Cheng-Pursoff equation [$K_i = IC_{50}/(1 + S/K_m)$]. Kinase assays were also performed using the Kinase Luminescent Assay Kit (Promega), following the manufacturer's instructions, and gave comparable results.

*Ld*GSK-3s activity (purified from *L. donovani* over-expressing transfectants, 1 μg enzyme/reaction) was also determined using potential protein substrates: *L. infantum* histone H1 (LeishH1),

mammalian histone H1 (Sigma), axin (recombinant, purified from bacteria), myelin basic protein and casein (dephosphorylated from bovine milk, Sigma), (approximately 1 μg substrate/reaction). LeishH1 was expressed in bacteria as a fusion protein with GST and purified with Sepharose 4B-Glutathione beads as previously described (Smirlis et al., 2006). LeishH1 recombinant protein was cleaved from the GST moiety by thrombin treatment (Smirlis et al., 2006). In vitro phosphorylation of protein substrates was performed in the kinase assay buffer. After 30-min incubation at 30 °C, in the presence of [γ-^{32}P] ATP (6000 Ci/mmol, 10 mCi/ml) in a final volume of 30 μl, the kinase reaction was stopped by addition of Laemmli buffer (Meijer et al., 2004). The protein substrates were resolved by 12% SDS–PAGE, stained with Coomassie blue and their phosphorylation level was visualised by autoradiography.

2.13. Homology modelling

The homology model of parasite GSK-3s was based on the crystal structure of the human GSK-3β complexed with 6-BIO (pdb 1Q41) and the respective of CRK3 on the template structure of human CDK2-cyclin A (pdb 1E9H), (Davies et al., 2001). Model building was performed with MODELLER v. 6 program (Sali and Blundell, 1993) and stereochemical validation with PROCHECK program (Laskowski et al., 1991). Docking was performed with a Monte Carlo search algorithm. Ligand partial charges were calculated in a semi-empirical level by MOPAC6 (AM1 hamiltonian) (Stewart, 1990).

3. Results

3.1. Evaluation of the antileishmanial effect of indirubins on L. donovani promastigotes and amastigotes

The Alamar blue assay (Mikus and Steverding, 2000), in a 96-well format, was used for the primary screening and subsequent monitoring of the growth of *L. donovani* promastigotes and axenic amastigotes exposed to indirubins. The same assay was adapted and used for estimating the growth of intracellular amastigotes 48 h after lysis of the infected macrophages treated for 72 h with the indirubins. In the initial screening, 16 indirubins were tested at 10 μM. Nine of the compounds did not significantly affect parasite growth even when used at a higher concentration of 50 μM. Four out of the 16 compounds tested significantly inhibited *Leishmania* growth and their IC_{50} values were determined, (Table 1). More specifically, 6-BIO, 6-BIA and 5-Me-6-BIO inhibited promastigote growth with an IC_{50} of 0.8 ± 0.1, 0.9 ± 0.1 and 1.2 ± 0.2 μM, respectively (Table 1). 5-BIO inhibited promastigote growth with an IC_{50} of 5.2 ± 1.6 μM (Table 1). Interestingly, 6-BIO, 6-BIA, 5-Me-6-BIO and 5-BIO were also found to significantly inhibit the growth of both *L. donovani* intracellular and axenic amastigotes with IC_{50} values ranging from 0.75 ± 0.05 to 1 ± 0.2 μM, respectively (Table 1). N1-methyl derivatives of 6-BIO and 6-BIA did not inhibit the growth of either promastigotes or amastigotes, consistent with the inactivation of indirubins as kinase inhibitors by this modification (Meijer et al., 2003).

All four compounds did not affect the growth of macrophages at the concentration used, but as determined using the same assay, they were toxic for host cells at significantly higher concentrations (IC_{50} values >25 μM). Amphotericin B used as a reference drug inhibited promastigote and amastigote (intracellular or axenic) growth with IC_{50} values of 0.1 ± 0.01 and 0.2 ± 0.02 μM, respectively.

3.2. Molecular characterisation of LdGSK-3s: expression and localisation in the L. donovani life cycle

Since 6-bromo indirubins are powerful and selective inhibitors of mammalian GSK-3 (Meijer et al., 2003; Polychronopoulos et al., 2004) we searched in the *Leishmania GeneDB* database for GSK-3 homologues (Parsons et al., 2005). Two GSK-3 encoding genes were found in the *Leishmania* genome using BLAST homology searches, a short and a long version. Comparison of the amino acid identities of the two human GSK-3 orthologues versus the two *L. infantum* forms revealed that GSK-3s is closer than GSK-3l to human GSK-3α and GSK-3β. However, GSK-3s has a slightly higher identity to GSK-3β than to GSK-3α (Table 2). This does not allow us to unambiguously determine whether GSK-3s is equivalent to the GSK-3β mammalian form.

Table 2
Amino-acid identity (%, above diagonal) and similarity (%, below diagonal) relationships of *Leishmania infantum* GSK-3 enzymes versus human and *Trypanosoma brucei* proteins[a].

	H.sap GSK-3β	*H.sap* GSK-3α	*L.inf* GSK-3s	*L.inf* GSK-3l	*T.bru* GSK-3s	*T.bru* GSK-3l
H.sap GSK-3β		67.1	39.5	22	40.7	32.2
H.sap GSK-3α	74.4		34.3	21.5	35.4	30.5
L.inf GSK-3s	55.8	48.1		19.5	65.4	29.8
L.inf GSK-3l	30.5	30.6	29.2		20.1	26.5
T.bru GSK-3s	55.9	48.1	80.6	27.9		31.2
T.bru GSK-3l	47.8	45.7	43.1	36.4	44.7	

[a] The table was constructed using BioEdit 7.0.5.3 Sequence Alignment Editor (pairwise global alignments using BLOSUM62 similarity matrix). Accession numbers for the enzymes were: *Homo sapiens* (*H.sap*) GSK-3β (P49841), *H. sapiens* GSK-3α (P49840), *L. infantum* (*L.inf*) GSK-3s (XP_001464844, LinJ18_V3.0270), *L. infantum* GSK-3l (XP_001465568, LinJ22_V3.0370), *T. brucei* (*T.bru*) GSK-3short (Tb10.61.3140), *T. brucei* GSK-3long (Tb927.7.2420).

We focused on the GSK-3s isoform for further studies, since: (i) the GSK-3s homologues are almost identical in different *Leishmania* species, and (ii) GSK-3s is slightly closer to the mammalian GSK-3β, the most well-studied isoform. The *GSK-3s* gene in *L. infantum*, in *L. major* and in *L. mexicana* is located on chromosome 18 and encodes a protein of 355 amino acids with a predicted molecular mass of 40.7 kDa. BLASTP analysis showed that the identified *L. donovani GSK-3s* gene was identical to the *L. infantum GSK-3* short gene and almost identical to *L. major* and *L. mexicana GSK-3* short and *GSK-3β* genes, respectively (98% identity and 99% similarity), (Supplementary Fig. S2). *Ld*GSK-3s shares 49% sequence identity and 68% similarity with hGSK-3β. It also shares 65% identity and 80% similarity with *T. brucei* GSK-3 "short", 47% identity and 67% similarity with *Danio rerio* GSK-3β, 42% identity and 64% similarity with *Plasmodium falciparum* GSK-3, and 49% identity and 68% similarity with *Mus musculus* GSK-3β (Supplementary Fig. S2).

*Ld*GSK-3s was detected in *L. donovani* extracts using an affinity-purified anti-*Ld*GSK-3s polyclonal antibody (raised against the recombinant protein expressed in *E.coli*) and a commercially available polyclonal anti-ratGSK-3β antibody (raised against the C-terminal sequence of rat GSK-3β). The ~40 kDa protein detected by both antibodies is in line with the predicted molecular mass of *Ld*GSK-3s. Western blot analysis indicated that the level of expression of *Ld*GSK-3s in *L. donovani* stationary and logarithmic-phase promastigotes (10^7 cells/lane) was comparable (Fig. 1A, lanes S and L, respectively). *Ld*GSK-3s was also detected in spleen-derived *L. donovani* amastigotes and axenic amastigotes (10^7 cells/lane), (Fig. 1A, lanes Am and Ax, respectively). Scanning densitometry of the detected bands revealed that *Ld*GSK-3s expression level was about 3-fold lower in amastigotes. As a control for loading equal number of cells, the blot was stripped and re-probed with the antiserum against *L. infantum* myo-inositol-1-phosphate synthase (*Lin*INO1), a 46 kDa protein whose level of expression is constitutive during promastigote growth and which is equally expressed in promastigotes and amastigotes, (Ilg, 2002; Rosenzweig et al., 2008) (Fig. 1B). No protein band was detected when pre-immune serum was used as a negative control (Fig. 2C, lane S, Ax). *Ld*GSK-3s was also recognised by the anti-ratGSK-3β antibody (Fig. 2D, lane S). Similarly, the mouse

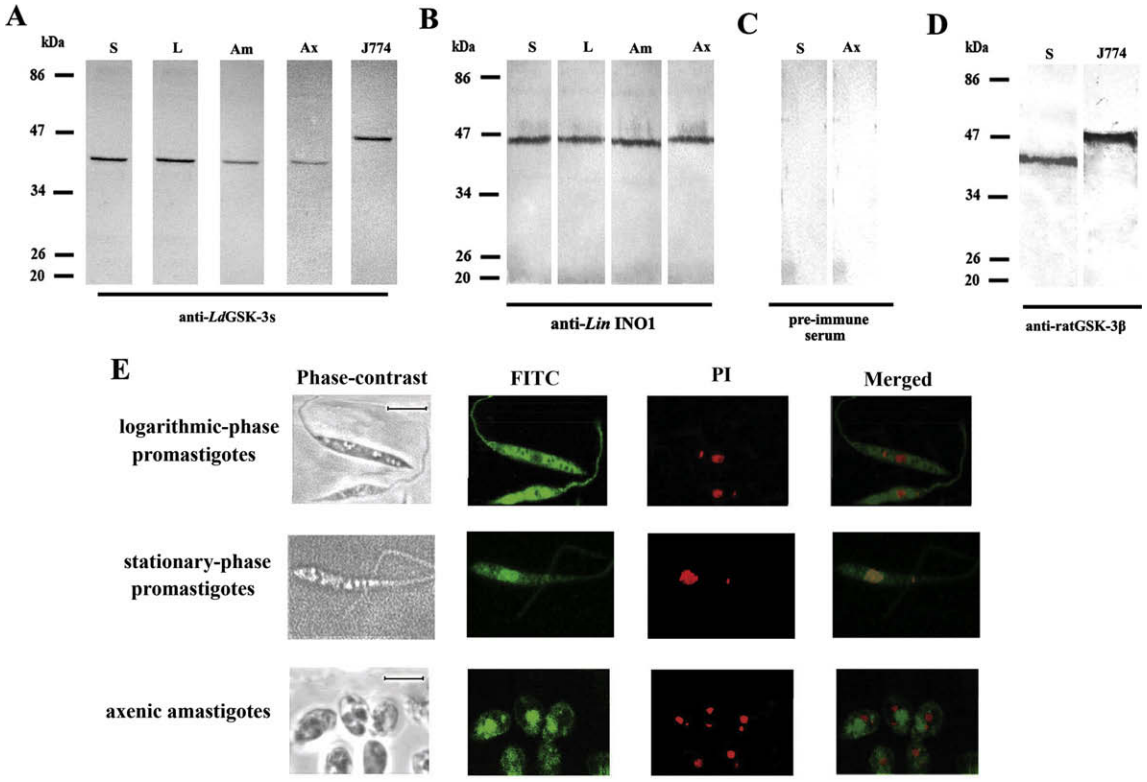

Fig. 1. *Leishmania donovani* glycogen synthase kinase-3 short (*Ld*GSK-3s) expression in *L. donovani*. Western blot analysis (A) anti-*Ld*GSK-3s antibody: stationary-phase promastigotes (S), logarithimic-phase promastigotes (L), axenic amastigotes (Ax), spleen-derived amastigotes (Am) and J774 macrophages (J774) 10^7 parasites or 9×10^5 macrophage cells were loaded per lane. (B) anti-*Lin*INO1 antibody, to confirm equal cell loading. (C) Pre-immune serum: stationary-phase promastigotes (S) and axenic amastigotes (Ax). (D) anti-ratGSK-3β antibody: stationary-phase promastigotes (10^7) and J774 cell extracts (9×10^5 cells/lane), used as positive controls. Evaluation of the level of expression of *Ld*GSK-3s was analysed using the Alpha Imager Software and compared with that of INO1. (E) Localisation of *Ld*GSK-3s in *L. donovani* logarithmic and stationary-phase promastigotes and logarithmic-phase axenic amastigotes, using the affinity-purified anti-*Ld*GSK-3s antibody (5 μg/ml). Parasite nuclei and kinetoplasts were counterstained with propidium iodide (PI). Scale bars 4 μm.

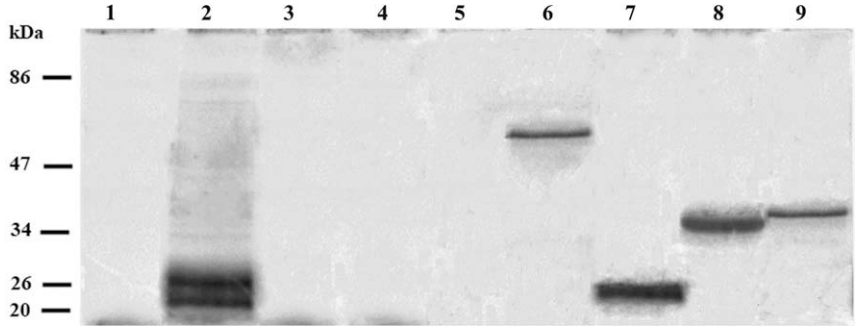

Fig. 2. Kinase activity of *Leishmania donovani* glycogen synthase kinase-3 short (*Ld*GSK-3s) purified from *L. donovani* over-expressing transfectants. The ability of *Ld*GSK-3s (1 μg *Ld*GSK-3s/reaction) to phosphorylate various substrates was assessed in vitro. Kinase reactions, containing approximately 1 μg substrate/reaction, were subjected to SDS–PAGE and phosphorylated substrates detected by autoradiography. Lane 1, *Ld*GSK-3s; lane 2, *Leishmania* histone H1 (LeishH1); lane 3, LeishH1 plus 4 μM 6-Br-5methylindirubin-3′oxime (5-Me-6-BIO); lane 4, LeishH1 plus the *Ld*GSK-3s kinase-dead mutant (*Ld*GSK-3s/K49R); lane 5, GST; lane 6, axin; lane 7, myelin basic protein, MBP; lane 8, mammalian histone H1 and lane 9, casein.

GSK-3β (a 47 kDa protein) in J774 cell extracts (9×10^5 cells/lane) was detected using both antibodies (Fig. 1A and D, lane J774). This result shows the cross-reactivity of the two antibodies with mammalian and leishmanial GSK-3s.

The intracellular localisation of *Ld*GSK-3s in *L. donovani* promastigotes and axenic amastigotes was detected by immunofluorescence using both the affinity-purified anti-*Ld*GSK-3s and the anti-ratGSK-3β antibodies. Immunostaining of *L. donovani* logarithmic-phase promastigotes showed that *Ld*GSK-3s is localised in the parasite cytoplasm and flagellum (Fig. 1E). FITC-staining in the parasite nucleus or kinetoplast was detected at background levels. Interestingly, *Ld*GSK-3s was localised mainly in the parasite nucleus and flagella in stationary-phase promastigotes (Fig. 1E). *Ld*GSK-3s was also detected in logarithmic-phase axenic amastigotes but the pattern of immunostaining was different from both logarithmic- and stationary-phase promastigotes: more condensed and localised immunostaining in the cytoplasm of axenic amastigotes (Fig. 1E). In all cases staining with the two antibodies was similar and therefore only that with the affinity-purified anti-*Ld*GSK-3s is shown.

Table 3
Inhibition of *Leishmania donovani* glycogen synthase kinase-3 short (*Ld*GSK-3s) and cdc-2 related kinase 3 (CRK3) kinase activities by indirubins[a].

Compounds	IC_{50} (μM)	
	*Ld*GSK-3s	CRK3
5-BIO	0.35	0.7
6-BIO	0.15	0.02
N-Methyl-6-BIO	>10	>10
6-BIA	0.17	0.25
N-Methyl-6-BIA	>10	>10
5-Me-6-BIO	0.09	0.65
6-FIO	3.3	0.4
6-ClIO	0.2	0.04

[a] *Ld*GSK-3s and CRK3 were assayed for their ability to phosphorylate GS-1 peptide and mammalian histone H1, respectively, in the presence of increasing concentrations of compounds. IC_{50} values were determined from dose–response curves and are expressed in μM.

3.3. LdGSK-3 s and CRK3 inhibitor screen

Since 6-bromo indirubins are powerful inhibitors of mammalian CDKs and GSK-3 (Meijer et al., 2003; Polychronopoulos et al., 2004) we thought to examine whether they also target *Ld*GSK-3s and/or CRK3. To this end we have purified *Ld*GSK-3s and CRK3 from *L. donovani* over-expressing transfectants and transgenic *L. mexicana* promastigotes, respectively (Supplementary Fig. S1) and their kinase activities were assayed using GS-1 peptide and histone H1 as substrates, respectively, in the presence of the indirubins that displayed maximum growth inhibition in the cell-based assay. Of note is that *L. donovani* CRK3 displays 99% sequence identity with *L. mexicana* CRK3, which was used for the inhibitor screen. Specific activities of the enzymes were found to be 800 U/mg for *Ld*GSK-3s and 750 U/mg for CRK3. After determining the K_m values of both kinases for ATP and their respective substrates, (Supplementary Fig. S3), dose–response curves were used to calculate the IC_{50} values (Table 3). 6-BIO, 6-BIA, 5-BIO and 5-Me-6-BIO inhibited *Ld*GSK-3s with IC_{50} values of 0.15, 0.17, 0.35 and 0.09 μM, respectively, whereas CRK3 was inhibited with IC_{50} values of 0.02, 0.25, 0.7 and 0.65 μM, respectively (Table 3). Thus, 5-Me-6-BIO displayed an approximately 7-fold selectivity for *Ld*GSK-3s over CRK3, whilst 6-BIO was about 7-fold more active towards CRK3 than *Ld*GSK-3s. 6-BIA inhibited CRK3 ~1.5-fold more than *Ld*GSK-3s. N1-methyl derivatives of 6-BIO and 6-BIA, which displayed no growth inhibition in the cell-based assay, were inactive on both kinases (Table 3).

To compare the inhibitory activity of indirubins against *Ld*GSK-3s and CRK3, IC_{50} values were evaluated relatively to K_i values of the inhibitors which were equal to ½ of IC_{50} values because kinase assays were performed in ATP concentration equal to the K_m for ATP. 5-Me-6-BIO inhibited *Ld*GSK-3s with a K_i of 0.045 μM and CRK3 with a K_i of 0.325 μM. 6-BIO inhibited *Ld*GSK-3s with a K_i of 0.075 μM and CRK3 with a K_i of 0.01 μM.

Indirubins 6-FIO, 6-ClIO and 6-IIO substituted at position 6 with the halogens F, Cl and I, respectively, were found less active towards both kinases (Table 3) as well as towards *L. donovani* promastigotes (IC_{50} values > 3 μM). Interestingly, 6-iodo substituted indirubin was 5-fold more active towards *Ld*GSK-3s.

3.4. Substrate selectivity of LdGSK-3s

Substrate selectivity of *Ld*GSK-3s purified from *L. donovani* over-expressing transfectants (1 μg *Ld*GSK-3s/reaction) was investigated using potential substrates: LeishH1, axin, myelin basic protein (MBP), mammalian histone H1 and casein (Fig. 2). LeishH1 was chosen because it possesses the consensus recognition motif for phosphorylation by GSK-3β: S/TXXXS/T(P), where X is any amino-acid (Doble and Woodgett, 2003). *Ld*GSK-3s shows no autophosphorylation when the kinase assay is performed without substrate (Fig. 2, lane 1). Phosphorylation of LeishH1 by *Ld*GSK-3s (Fig. 2, lane 2) was inhibited when the kinase reaction was performed in the presence of 4 μM 5-Me-6-BIO, (Fig. 2, lane 3). Control kinase reaction was also performed, using the kinase-dead mutant *Ld*GSK-3s/K49R with LeishH1 as a substrate (Fig. 2, lane 4). The GST moiety was not phosphorylated by *Ld*GSK-3s (Fig. 2, lane 5). Axin (~55 kDa), MBP (18.4 kDa), mammalian histone H1 (21.5 kDa) and casein (23 kDa) were found to be good protein substrates of *Ld*GSK-3s (Fig. 2, lanes 6–9). The basic nature of histones and the rich content in prolines in casein that affects its conformation cause them to migrate slower in SDS–PAGE. None of the substrates tested displayed intrinsic phosphorylation (data not shown). However, more experimental data is needed to prove in vivo interaction of *Ld*GSK-3s and LeishH1, as the kinase phosphorylating LeishH1 has not been identified so far.

3.5. Cell-cycle disruption and induction of apoptosis-like death in 5-Me-6-BIO- and 6-BIO-treated L. donovani promastigotes

The cell-cycle distribution of promastigotes incubated with 5-Me-6-BIO and 6-BIO was analysed using flow cytometry (Fig. 3A). Promastigotes treated with 1 μM 5-Me-6-BIO for either 24 or 48 h resulted in a decrease in the G0/G1 DNA content (40.9% and 37.5%, respectively, compared with 66% of control parasites) and an increase in cells in S phase (13.4% and 11%, respectively, compared with 7.3% of control cells) with a concomitant increase in the G2/M phase of the cell-cycle (43.7% and 49.4%, respectively, compared with 23.9% of control cells). Treatment of promastigotes with 6-BIO resulted in an increase in the proportion of cells with G2/M DNA content, the latter being time- and dose-dependent. After 48 h of treatment with 2 μM 6-BIO 74.5% of cells were in G2/M (Fig. 3B). Control cells treated with the diluent (0.01% or 0.02% DMSO) had a normal cell-cycle distribution at all time-points studied (66% G0/G1, 7.66% S, 23.8% G2/M). Of note is that cells treated with 2 μM 5-Me-6-BIO for 24 and 48 h had a high percentage of hypodiploid cells (<2 N DNA content) and accumulated in the sub-G0 phase (29.8% and 40%, respectively) which is indicative of apoptotic-like cell death (Fig. 3A).

In order to investigate whether 5-Me-6-BIO- and 6-BIO- induced apoptotic-like mechanisms in *Leishmania* we used double staining with Annexin V-FITC and PI. This staining allows the differentiation between early apoptotic (Annexin V-FITC positive), late apoptotic (Annexin V-FITC and PI positive), necrotic (PI positive) and viable cells (unstained). Incubation of cells with 0.02% DMSO showed negative staining for both Annexin V and PI, as 97.8% of cells were viable at all time-points (Fig. 3C, control). In the positive control for necrosis, 39.23% of Triton X-100-treated promastigotes were found to be PI positive (Fig. 3C, Triton X-100). In the positive control for apoptosis, 49.23% of cells treated with 4 mM hydrogen peroxide (H_2O_2) for 40 min (Das et al., 2001) were found to be late apoptotic, 2.97% early apoptotic and 13.99% necrotic (Fig. 3C, H_2O_2). Treatment of promastigotes with 2 μM 5-Me-6-BIO for 48 h resulted in a high percentage of Annexin V positive cells (57.9%), of which 6.42% were early apoptotic and 51.48% were late apoptotic, whilst viable cells were 38.42% (Fig. 3C, 5-Me-6-BIO). The percentage of cells undergoing early apoptosis was higher than that of late apoptosis (29.35% versus 12.03%) when cells were treated for 24 h whereas treatment of promastigotes with 2 μM 5-Me-6-BIO for 72 h resulted in an increase in PI positive cells, as 26.04% of cells were necrotic and 61.2% late apoptotic, whilst only 10.83% of cells were viable (data not shown). Treatment of promastigotes with 2 μM 6-BIO for 48 h resulted in an

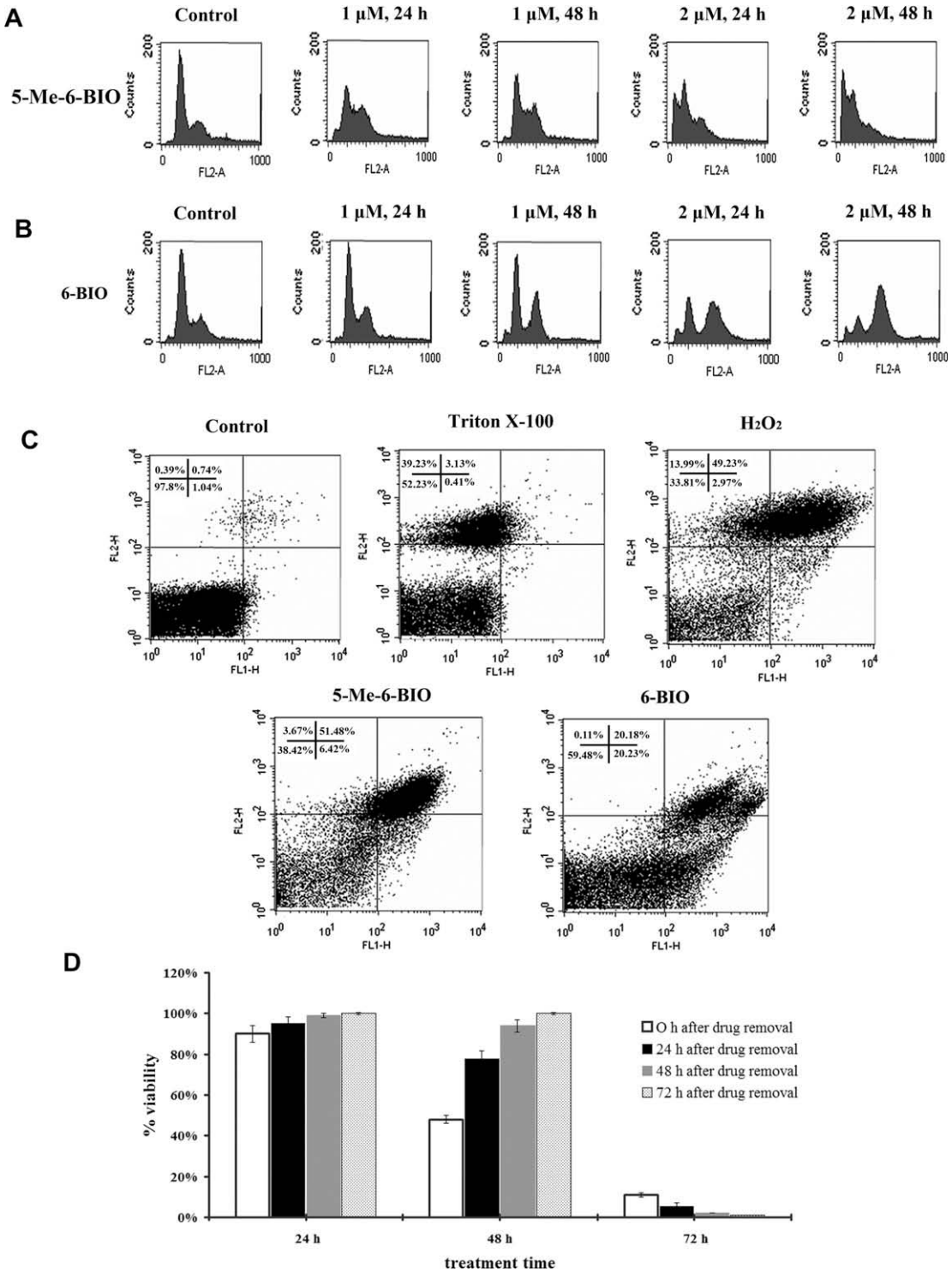

Fig. 3. Effects of indirubins on cell-cycle progression and apoptosis-like cell death. Flow cytometry was used to assess the cell-cycle status of *Leishmania donovani* promastigotes exposed to indirubins in vitro. (A) Stationary-phase promastigotes were seeded at 1×10^6 cells/ml and incubated in the presence of 6-Br-5methylindirubin-3′oxime (5-Me-6-BIO) (1 or 2 μM) or DMSO (control), for 24 or 48 h or (B) 6-BIO (1 or 2 μM) or DMSO (control), for 24 or 48 h. (C) *L. donovani* promastigotes were incubated with 2 μM 5-Me-6-BIO, 2 μM 6-BIO or DMSO (Control) for 48 h and then stained with Annexin V-FITC and propidium iodide (PI) to assess phosphatidylserine translocation and membrane integrity. Promastigotes were also incubated with either 4 mM H_2O_2 for 40 min (apoptosis positive control) or 0.1% Triton X-100 for 5 min (necrosis positive control). Flow cytometry was performed using a FACSCalibur and data analysed using the Cell Quest software. The percentage of cells in each quadrant represent the following: lower left, double negative; upper left, PI single positive; lower right, Annexin V single positive and upper right, PI-Annexin V double positive. Results are representative of three independent experiments. (D) *L. donovani* promastigotes were incubated with 2 μM 5-Me-6-BIO for 24, 48 and 72 h. At these time-points (white bars/0 h), drug was removed followed by further incubation of cells in drug-free medium for 24 h (black bars), 48 h (grey bars) and 72 h (dotted bars). The percentages of cell viability were determined using the trypan blue exclusion test. Error bars represent the SDs of three independent experiments.

increased labelling with Annexin V. Early and late apoptotic cells together constituted about 40.4% of the cells: 20.18% of cells were late apoptotic and 20.23% were early apoptotic compared with controls (Fig. 3C, 6-BIO).

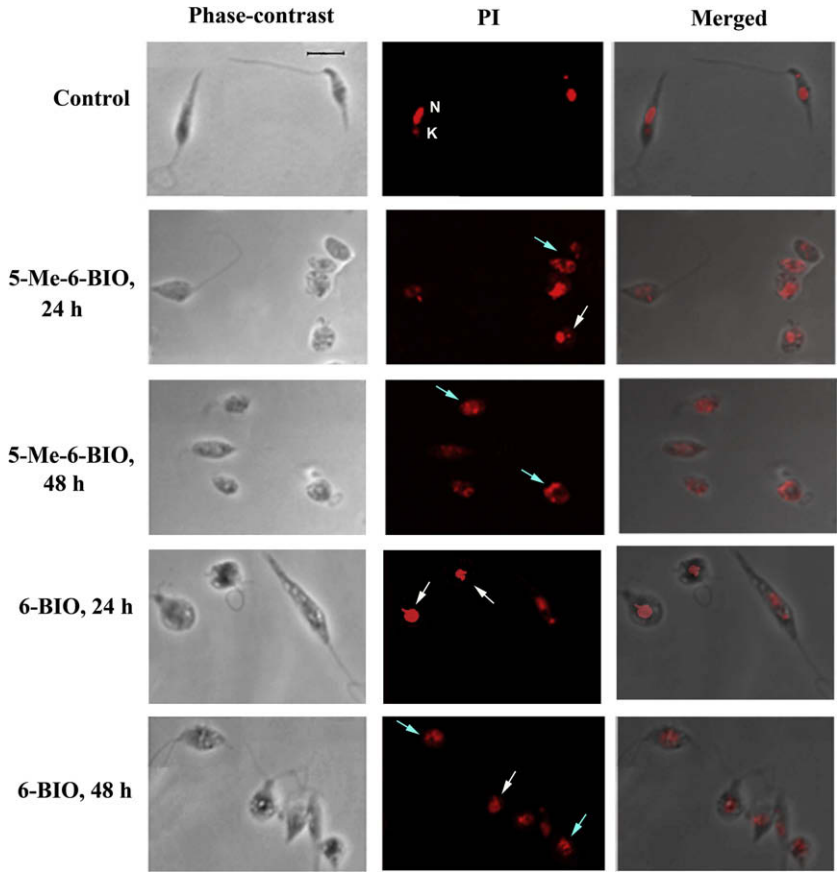

Fig. 4. Cell and nuclear morphology of *Leishmania donovani* promastigotes exposed to indirubins. *Leishmania donovani* promastigotes were incubated with 2 μM 6-Br-5methylindirubin-3′oxime (5-Me-6-BIO), 2 μM 6-BIO or 0.02% DMSO (control) for 24 and 48 h, in vitro, and then fixed and stained with propidium iodide. Confocal micrographs are representative of three independent experiments. Scale bar 4 μm. N, nucleus; K, kinetoplast; white arrows indicate condensed nuclei; blue arrows indicate disintegrated nuclei.

To further study whether the observed effect of indirubins was due to apoptosis-like death we monitored morphological and nuclear changes by confocal microscopy. Control cells displayed a normal elongated morphology with two discrete stained organelles, the nucleus and the kinetoplast (Fig. 4, control). Promastigotes exposed to 5-Me-6-BIO for 24 h showed rounded forms, cell shrinkage and variations in the length of their flagella as well as nuclear changes characteristic of apoptosis-like death; apoptotic nuclei were identified by their bright red fluorescence, which included a certain degree of condensation of nuclear chromatin in 36% of cells and breakdown of the nuclear material in 41% of cells (Fig. 4, 5-Me-6-BIO, 24 h). At the 48 h-time point, 78% of cells exhibited a totally fragmented nucleus (Fig. 4, 5-Me-6-BIO, 48 h). Formation of zoids was not observed (Grant et al., 2004). Treatment with 2 μM of 6-BIO for 24 h had less pronounced morphological alterations. It resulted in cells with either a normal morphology with a discrete kinetoplast and a nucleus (approximately 38% of cells) or in rounded-shaped with short flagella and condensed nuclear chromatin (~62%) (Fig. 4, 6-BIO, 24 h). After treatment with 6-BIO for 48 h, the majority of parasites (75%) displayed an aberrant morphology, with round body shape and short flagella of which 36% displayed nuclear condensation and 39% nuclear fragmentation (Fig. 4, 6-BIO, 48 h).

Since the cellular effects induced by 5-Me-6-BIO were more pronounced than those of 6-BIO we investigated whether they were reversible after drug removal. To this end the recovery of cells following exposure to 5-Me-6-BIO for 24, 48 and 72 h was assessed 24, 48 and 72 h after the drug removal. Control cells treated with 0.02% DMSO were viable at all time-points tested (100% viability). As shown in Fig. 3D treatment of cells with 5-Me-6-BIO for 24 h followed by incubation with fresh medium up to 72 h resulted in full recovery of cells. After 48 h of treatment, about 48% of cells were viable. Further incubation in fresh medium for 24 h resulted in an increase in the percentage of viable cells (77.7%). At the 48 h and 72 h time-points, a full recovery of the cells was observed. In contrast, incubation for 72 h with 5-Me-6-BIO resulted in about 89% dead cells. Removal of the drug resulted in irreversible cytotoxicity.

3.6. LdGSK-3s over-expression in L. donovani counteracts 5-Me-6-BIO- and 6-BIO-induced growth inhibition, cell-cycle progression and apoptosis-like death

To investigate whether *Ld*GSK-3s is the intracellular target of 5-Me-6-BIO and whether all the observed phenotypes in the presence of 5-Me-6-BIO could be attributed to inhibition of this kinase, we have generated transgenic *L. donovani* promastigotes over-expressing *Ld*GSK-3s and compared their susceptibility to 5-Me-6-BIO with that of control transfectants bearing the plasmid alone. We also investigated whether over-expression of *Ld*GSK-3s affected the growth inhibitory effect of 6-BIO. As a control, we generated transgenic promastigotes overexpressing *Ld*GSK-3s/K49R, which was a kinase-dead mutant as confirmed by kinase assays (Fig. 2, lane 4). The mutation of the catalytic residue Lys 49 to Arg was designed based on the homology model of *Ld*GSK-3s and on the widely used mutation of Lys 85 to Arg or Ala of mammalian

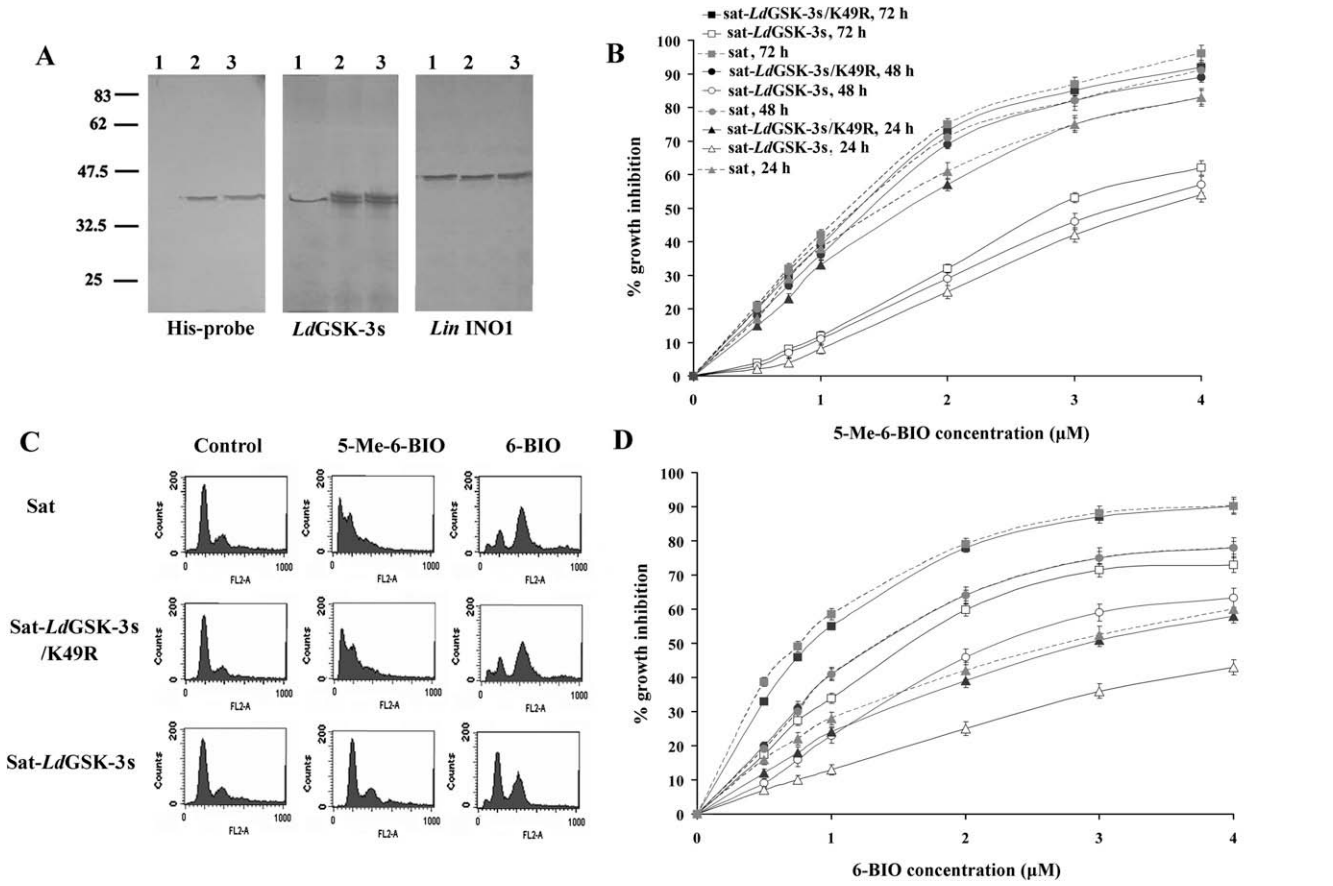

Fig. 5. Over-expression of *Leishmania donovani* glycogen synthase kinase-3 short (*Ld*GSK-3s) counteracts the effects of 6-Br-5methylindirubin-3′oxime (5-Me-6-BIO) and 6-BIO on *Leishmania donovani* promastigotes. (A) Western blot analysis of *L. donovani* sat, sat-*Ld*GSK-3s/K49R and sat-*Ld*GSK-3s promastigotes (10^7/lane) probed with His-probe, anti-*Ld*GSK-3s or anti-*Lin*INO1 antibodies. The intensity of the bands was analysed with the use of the Alpha Imager Software and the fold-over-expression estimated. (B) Growth inhibition of *L. donovani* sat (grey symbols, dotted lines), sat-*Ld*GSK-3s/K49R (solid symbols) and sat-*Ld*GSK-3s (open symbols) transfectants treated with different 5-Me-6-BIO concentrations after 24, 48 and 72 h of incubation. Results are depicted from four independent experiments performed in duplicate. (C) Flow cytometry analysis of *L. donovani* sat, sat-*Ld*GSK-3s/K49R and sat-*Ld*GSK-3s transfectants incubated in the presence of 0.02% DMSO (control) or 2 μM 5-Me-6-BIO or 2 μM 6-BIO for 48 h. Results are indicative of three independent experiments. (D) Growth inhibition of *L. donovani* sat (grey symbols, dotted lines), sat-*Ld*GSK-3s/K49R (solid symbols) and sat-*Ld*GSK-3s (open symbols) transfectants treated with different 6-BIO concentrations after 24, 48 and 72 h of incubation. Results are depicted from four independent experiments performed in duplicate.

GSK-3β, which results in a kinase-dead protein (He et al., 1995). Over-expression of *Ld*GSK-3s and expression of *Ld*GSK-3s/K49R in the *Ld*GSK-3s and *Ld*GSK-3s/K49R transfectants was confirmed by immunoblotting using both a His-probe antibody and the anti-*Ld*GSK-3s antibody (Fig. 5A). The *Lin*INO1 antibody was used as a loading control. Scanning densitometry showed that the level of expression of *Ld*GSK-3s in *Ld*GSK-3s and *Ld*GSK-3s/K49R transfectants was about 2-fold higher in comparison with sat transfectants (Fig. 5A). Expression of the kinase-dead mutant did not cause any apparent changes in parasite growth or morphology.

The susceptibility of stationary-phase *L. donovani* sat, sat-*Ld*GSK-3s and sat-*Ld*GSK-3s/K49R transfectants to increasing concentrations of 5-Me-6-BIO was assessed after 24, 48 and 72 h of treatment by cell counting. The IC_{50} of 5-Me-6-BIO after 24, 48 and 72 h of treatment of the sat-transfectants was 1.5 ± 0.2, 1.25 ± 0.1 and 1.2 ± 0.1 μM, respectively, which are comparable with the IC_{50} against wild-type promastigotes (Table 1), whereas its respective IC_{50} for the *Ld*GSK-3s over-expressing transfectants was 3.6 ± 0.3, 3.2 ± 0.2 and 2.8 ± 0.2 μM (Fig. 5B). As expected, the sat-*Ld*GSK-3s/K49R transfectants were inhibited by 5-Me-6-BIO with IC_{50} values of 1.7 ± 0.1 μM after 24 h, 1.4 ± 0.1 μM after 48 h and 1.3 ± 0.05 μM after 72 h, which are comparable with the respective IC_{50} values against sat-transfectants (Fig. 5B).

Treatment of the *Ld*GSK-3s over-expressing transfectants with 6-BIO resulted in a clear decrease in their sensitivity, with IC_{50} values of 4.8 ± 0.5 μM after 24 h, 2.2 ± 0.4 μM after 48 h of treatment and 1.57 ± 0.3 μM after 72 h of treatment, which were approximately 2-fold higher compared with IC_{50} values of sat and sat-*Ld*GSK-3s/K49R transfectants (Fig. 5D). Sat and sat-*Ld*GSK-3s/K49R transfectants treated with different 6-BIO concentrations displayed growth inhibition with approximately the same IC_{50} values as *L. donovani* wild-type promastigotes. Sat transfectants were inhibited with IC_{50} values of 2.75 ± 0.45 μM after 24 h of treatment, 1.3 ± 0.3 μM after 48 h of treatment and 0.78 ± 0.25 μM after 72 h of treatment and sat-*Ld*GSK-3s/K49R transfectants were inhibited with IC_{50} values of 2.9 ± 0.3 μM after 24 h, 1.3 ± 0.2 μM after 48 h and 0.8 5 ± 0.2 μM after 72 h (Fig. 5D).

Flow cytometry analysis of the DNA content of control *L. donovani* sat, sat-*Ld*GSK-3s and sat-*Ld*GSK-3s/K49R over-expressing transfectants, treated with 0.02% DMSO, showed that cells had a normal cell-cycle distribution: 67.9% G1, 6.9% S, 23.2% G2 (Fig. 5C, control). Interestingly, sat-*Ld*GSK-3s promastigotes incubated with 2 μM 5-Me-6-BIO for 48 h had a normal cell-cycle distribution: 62% G1, 5.45% S and 30.5% G2 (Fig. 5C, 5-Me-6-BIO), whereas 40% of sat and sat-*Ld*GSK-3s/K49R transfectants were hypodiploid and accumulated in the sub-G0 phase (Fig. 5C), as was observed with wild-type promastigotes (Fig. 3A).

However, as shown in Fig. 5C, *Ld*GSK-3s over-expressing promastigotes treated with 6-BIO displayed a less pronounced increase in G2/M (41.7% compared with 74.5% in 6-BIO-treated wild-type parasites) and a less pronounced decrease in G0/G1 (46% compared with 15.8% in 6-BIO-treated wild-type parasites) (Fig. 5C, sat-*Ld*GSK-3s). In contrast, sat transfectants incubated with 2 μM 6-BIO for 48 h were comparable with wild-type promastigotes and arrested at G2/M (74.9% compared with 23.2% of control), with a significant decrease in G0/G1 (19.3% compared with 67.9% of control) (Fig. 5C, 6-BIO). Similar results with the latter were obtained for the sat-*Ld*GSK-3s/K49R transfectants which had the following cell-cycle distribution: 21.8% G0/G1, 4.4% S and 71.7% G2/M.

Since *Ld*GSK-3s over-expression resulted in a significantly reduced growth inhibition and a normal cell-cycle distribution upon 5-Me-6-BIO-treatment, we investigated whether *Ld*GSK-3s over-expression affected apoptosis-like death using the terminal deoxynucleotidyltransferase-mediated dUTP nick end labelling (TUNEL) assay, which detects apoptosis at a single-cell level. Control cells treated with 0.02% DMSO (sat, sat-*Ld*GSK-3s or sat-*Ld*GSK-3s/K49R) containing intact genomic DNA were not stained, (Fig. 6, control). Promastigotes treated with 4 mM H_2O_2 for 6 h, served as a TUNEL positive control, as about 99% of cells showed positive nuclear staining (Fig. 6, H_2O_2). Sat transfectants exposed to 2 μM 5-Me-6-BIO for 48 h were about 68% TUNEL positive and their morphology was dramatically affected in comparison to the normal elongated morphology of control cells (Fig. 6, sat/5-Me-6-BIO). Treated cells displayed an aberrant morphology, with round body shape and cell shrinkage. Sat-*Ld*GSK-3s transfectants treated with 2 μM 5-Me-6-BIO for 48 h were not positive for TUNEL reactivity, only a background staining of about 3% was detected and their morphology was not affected (Fig. 6, sat-*Ld*GSK-3s/5-Me-6-BIO). Sat-*Ld*GSK-3s/K49R transfectants were about 70.4% TUNEL positive (Fig. 6, sat-*Ld*GSK-3s/K49R/5-Me-6-BIO).

The contribution of *Ld*GSK-3s in the apoptosis-like death observed in 6-BIO treated promastigotes was also studied using the over-expressor lines. Whereas sat transfectants exposed to 2 μM 6-BIO for 48 h were ~50% TUNEL positive and their morphology was dramatically affected, *Ld*GSK-3s over-expressing transfectants were resistant to the effects of 6-BIO and displayed a much milder phenotype. Only 20% of the cells were TUNEL positive and their morphology was not significantly affected compared with control cells (Fig. 6, sat/6-BIO and sat-*Ld*GSK-3s/6-BIO, respectively). As expected, sat-*Ld*GSK-3s/K49R transfectants were about 52.9% TUNEL positive (Fig. 6, sat-*Ld*GSK-3s/K49R/6-BIO).

3.7. Structure activity relationships studies of indirubin-leishmanial kinases interactions using molecular simulations

Biological results imply that indirubins inhibit leishmanial kinases. Interestingly, the selectivity observed for 6-substituted indirubins towards GSK-3 with respect to the CDKs in human is reversed in the case of *Leishmania* and the homologous kinases (GSK-3 and CRK3) with the exception of the 6-iodo as well as the bisubstituted 5-Me-6Br analogues. Whilst indirubins potently inhibit the leishmanial GSK-3s (5-Me-6-BIO with an IC_{50} = 0.09 μM and 6BIO with an IC_{50} = 0.150 μM), they are not as efficient as in the case of the human homologue (5-Me-6-BIO with an IC_{50} = 0.006 μM and 6-BIO with an IC_{50} = 0.005 μM) (Meijer et al., 2003; Polychronopoulos et al., 2004).

Both pairs of homologous kinases are highly similar and the observed differences in affinity could possibly be explained by the key residue differences of the binding cavity. In order to obtain insight in the inhibitor–protein interactions, we built homology models of the parasite kinases (Supplementary Data S1). Despite the fact that important residues of the leishmanial GSK-3s seem to be well conserved (Supplementary Fig. S2), there were two major differences between the two kinases located in the binding pocket: (i) the replacement of $Gln185^{hGSK\text{-}3\beta}$ by $His155^{LGSK\text{-}3s}$ in the sugar-binding region, and (ii) the replacement of the "gatekeeper" $Leu132^{hGSK\text{-}3\beta}$ by $Met100^{LGSK\text{-}3s}$. The "gatekeeper" residue controls access to a hydrophobic cavity of the binding pocket and is considered as a selectivity determinant of most ATP competitive kinase inhibitors (Bohmer et al., 2003). In the majority of the members of the GSK-3 family (CMGC III), the gatekeeper is a leucine, except for MCK-1 kinase which has a methionine (Hanks and Quinn, 1991). However, a methionine is present in *Leishmania*, *T. brucei* and *P. falciparum* GSK-3s, (Supplementary Fig. S2).

Docking calculations were performed in order to study the binding mode/interactions of indirubins in the binding cavity of each kinase. In each case the inhibitor was anchored at the kinase backbone through the formation of three hydrogen bonds in the usually observed adenine type of interaction (Fig. 7A), whilst the substituent of position 6 was positioned in the hydrophobic cavity formed by the sidechain of the gatekeeper residue interacting with it. In human GSK-3β the leucine gatekeeper can form only hydrophobic interactions with the position 6 substituent of indirubin. However, in the parasite kinase the mode of interactions accommodated by the methionine gatekeeper is more complicated, resulting in a larger entropic and desolvation cost upon inhibitor binding (Supplementary Data S1). Such a net effect for the replacement of the leucine gatekeeper to a methionine could be considered as unfavourable for binding affinity, accounting for the loss of binding affinity in a common trend for all indirubins tested, which is in consistency with IC_{50} results obtained from kinase assays.

The higher affinity for CRK3 (reversal of selectivity with respect to the human kinases) demonstrated by 6-substituted indirubins tested with the exception of 6-IIO, 5-Me-6-BIO and partially of 6-BIA compared to the affinity for *Ld*GSK-3s could be explained by the formation of a hydrogen bond between $Tyr101^{CRK3}$ and $Glu103^{CRK3}$ (Fig. 7B), which is not possible in the human CDK2 homolog. The influence of this bonding interaction on the cavity size and subsequently on the ligand affinity could explain the observed gain of selectivity of 6-BIO towards CRK3. The above holds with the exception of 6-IIO, the bisubstituted 5-Me-6-BIO and the acetoxime 6-BIA, for which energy optimisation calculations demonstrated that the presence of the bulky substituent provoked a displacement of the ligand and the pair of residues Tyr101-Glu103 (Fig. 7C) resulting in less favorable interactions and loss of affinity.

All aforementioned structural observations are in accordance with previous studies showing that minor differences of the kinase binding cavity elements induce major variations in affinity and should be taken into account in designing new selective inhibitors of the leishmanial GSK-3s and CRK3. One possible route of selectively improving affinity towards the parasite GSK-3 is by taking advantage of the differential presence of the proton accepting $His155^{LGSK\text{-}3}$ (instead of $Gln185^{hGSK\text{-}3\beta}$ of human). The replacement or extension of the oxime by a group with the potential to form attractive albeit selective interactions with the sidechain of $His155^{LGSK\text{-}3}$ would increase affinity towards the parasite protein. Combined with the obvious preference of *Ld*GSK-3 for bisubstituted or generally bulkier substituents with regard to CRK3, a moderate selectivity improvement can be achieved, resulting in an increase of parasite killing whilst reducing toxicity to human cells.

4. Discussion

Herein we showed that three 6-bromo substituted indirubins, 6-BIO, 6-BIA and 5-Me-6-BIO were powerful inhibitors of both *L. donovani* promastigote and intracellular amastigote growth. *Leishmania donovani* axenic amastigotes were also inhibited by the

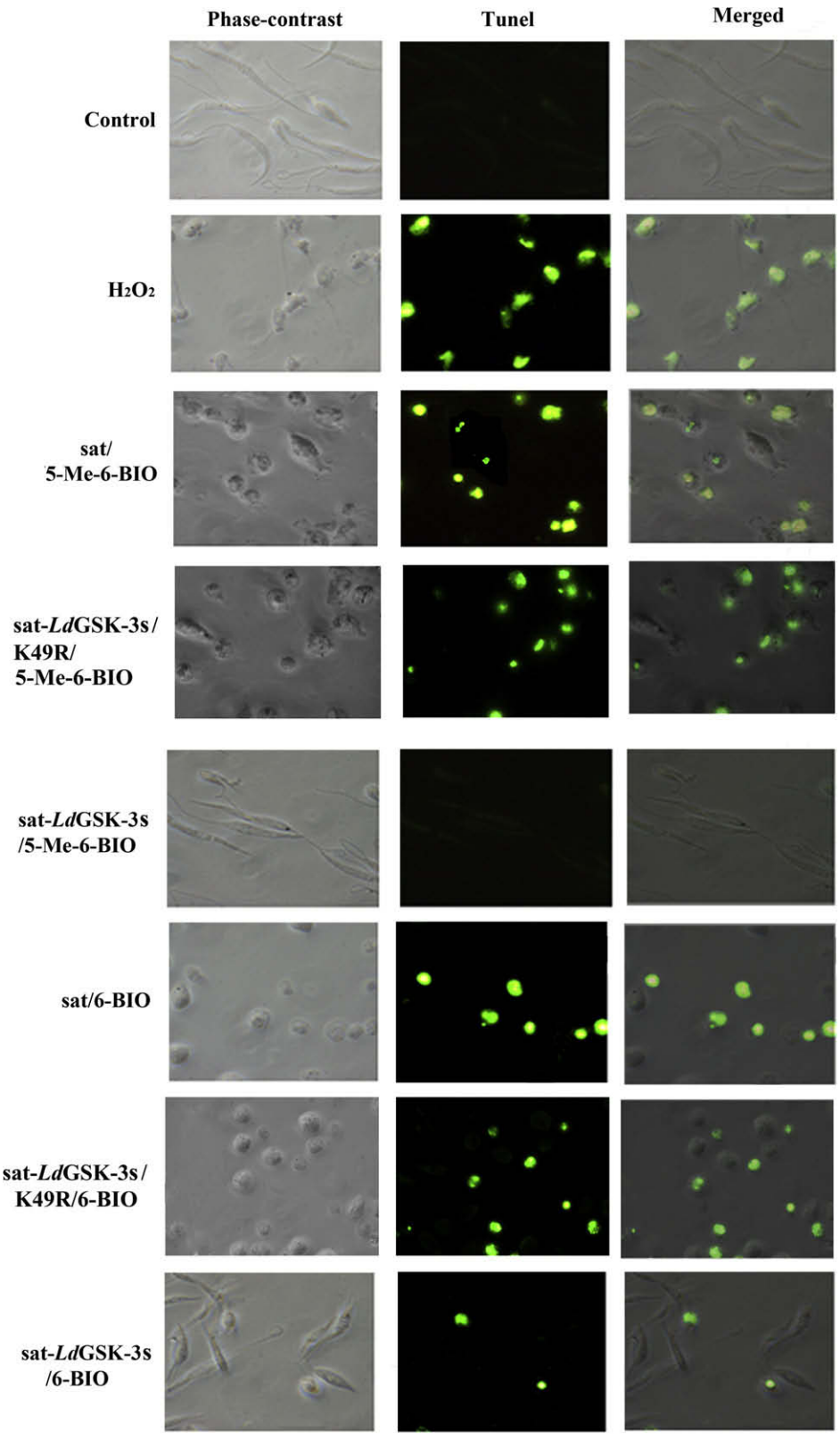

Fig. 6. DNA fragmentation in *Leishmania donovani* promastigotes incubated with indirubins. *Leishmania donovani* sat, *Ld*GSK-3s kinase-dead mutant (sat-*Ld*GSK-3s/K49R) and sat-*Ld*GSK-3s transfectants were incubated with 0.02% DMSO (negative control), 2 μM 6-Br-5methylindirubin-3′oxime (5-Me-6-BIO), 2 μM 6-BIO or 4 mM H_2O_2 (apoptosis positive control) and then subjected to the terminal deoxynucleotidyltransferase-mediated dUTP nick end labelling assay (TUNEL). Cells were visualised under a Zeiss fluorescence microscope at 120× magnification. The experiment was performed three times.

three indirubins with IC_{50} values $\leqslant 1$ μM, a finding that further supports that indirubin-induced growth inhibition of intracellular amastigotes is mediated through parasite-kinase(s) inhibition and not through inhibition of the host-kinase(s).

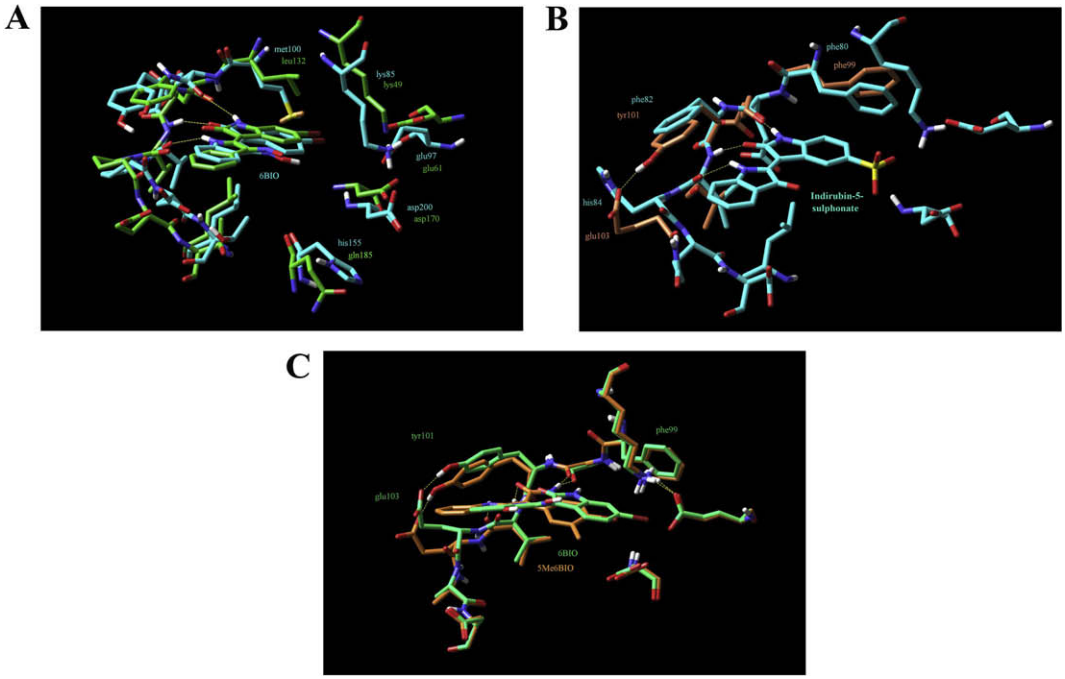

Fig. 7. Docking calculations showing the binding mode/interactions of indirubins in the binding cavity of each kinase. (A) A superposition of the crystal structure of human glycogen synthase kinase-3 (GSK-3) active site complexed with 6-Br-indirubin-3′oxime (6-BIO) (green) and the complex of *Leishmania donovani* glycogen synthase kinase-3 short (*Ld*GSK-3s) with 6-BIO resulting from docking calculations (turquoise). Hydrogen bonds are depicted as yellow dotted lines. Residues within the active site which differ between human and *L. donovani* GSK-3s are annotated, with the most important for 6-BIO affinity being the gatekeeper mutation of leucine132 in the human to methionine100 in the parasite protein. (B) Overlay of the crystal structure of cyclin-dependent kinase 2 (CDK2) complexed with indirubin-5-sulphonate (turquoise) and the cdc-2 related kinase 3 (CRK3) homology model (orange). The double mutation of phe82 in CDK2 to tyr101 in CRK3 and of his84 in CDK2 to glu103 in CRK3 results in a hydrogen bond between tyrosine and glutamate (shown in yellow) that translates the paired sidechains towards the cavity reducing its volume and offering a rigid partner for stacking or charge dipole stabilizing interactions with the extended aromatic scaffold of indirubins to form. (C) Ligands 6-BIO (green) and 5-Me-6-BIO (orange) in the CRK3 binding cavity as resulted from simple energy minimizations. Visible are the displacements of the bisubstituted 5-Me-6-BIO relative to 6-BIO and of the tyrosine-glutamate bonded pair.

The adapted Alamar blue assay allows the rapid and easy screening of the antileishmanial activity of compounds in 96-well format, although it is not very quantitative for measuring intramacrophage *Leishmania* growth compared with luciferase-expressing recombinant parasites (Roy et al., 2000). Also it does not measure the number of amastigotes at the point of lysis. However, contrary to Giemsa staining it takes into account only viable cells.

Since 6-bromo substitution on the indirubin backbone enhances the selectivity for mammalian GSK-3 over CDKs (Meijer et al., 2003) we investigated whether 6-BIO, 6-BIA and 5-Me-6-BIO target GSK-3 in *Leishmania a*nd studied their selectivity over CRK3. To this end we identified and characterised one of the two GSK-3 forms in *L. donovani*, namely *Ld*GSK-3s, and found that its expression pattern was comparable in logarithmic and stationary-phase promastigotes, but it was about 3-fold down-regulated in amastigotes, consistent with recent findings on *Ld*GSK-3s expression in *L. donovani* axenic amastigotes (Rosenzweig et al., 2008). In addition, *Ld*GSK-3s which had cytosolic and flagellar localisation in logarithmic-phase promastigotes, displayed nuclear translocation in stationary-phase promastigotes. In mammalian cells, GSK-3β is also predominately in the cytosol although under proapoptotic stimuli, a portion of GSK-3β is found within the nucleus (Meares and Jope, 2007). *Ld*GSK-3s translocation to the nucleus in stationary-phase promastigotes, thought to be arrested in G1 phase of the cell-cycle (Wiesgigl and Clos, 2001), may reflect a role for *Ld*GSK-3s in G1, consistent with accumulation of parasites in G1 when *Ld*GSK-3s is inhibited with 5-Me-6-BIO. The observed differences in the localisation and expression level of *Ld*GSK-3s may reflect divergent roles played by *Ld*GSK-3s in the two parasite stages. It could be speculated that in the intracellular amastigotes the function of *Ld*GSK-3s may be linked, among others, to their response and adaptation to stress conditions i.e. pH and temperature changes (Richard et al., 2005). The finding that the level of inhibition of promastigotes and amastigotes by 5-Me-6-BIO is the same although *Ld*GSK-3s is 3-fold less in amastigotes may suggest that *Ld*GSK-3s activity is higher in the latter or that 5-Me-6-BIO may also target other kinases in this stage.

Inhibitor screen assays against *Ld*GSK-3s and CRK3 showed that 5-Me-6-BIO, which is a 50-fold selective inhibitor of mammalian GSK-3 over CDK1/Cyclin B (Meijer et al., 2003; Polychronopoulos et al., 2004) displayed an approximately 7-fold selectivity for *Ld*GSK-3s over CRK3. However, 6-BIO was about 7-fold more active towards CRK3 than *Ld*GSK-3s, although it is a mammalian GSK-3 selective inhibitor, with 64-fold less potency towards CDK1/Cyclin B (Meijer et al., 2003). Molecular docking of the compounds in hGSK-3 and CDK1 active sites compared with *Ld*GSK-3s and CRK3 support the higher inhibitory activity of 5-Me-6-BIO towards *Ld*GSK-3s compared with CRK3 and the lower inhibitory activity of 6-BIO towards *Ld*GSK-3s compared with that against its mammalian counterpart.

5-Me-6-BIO and 6-BIO displayed a disparity between cellular activity and enzyme activity (K_i values) (22- to 27-fold for 5-Me-6-BIO and 75- to 80-fold for 6-BIO), which can be attributed to: (i) the ATP concentration in the kinase assays, that is several fold lower than the intracellular concentration, which is in the mM range, (ii) the bioavailability of the inhibitors (cell permeability of the compounds, rate of inhibitor efflux by cell efflux pumps), (iii) possible in vivo phosphatase activity, (iv) the intracellular concentration of the target kinase, (v) the presence of the *Ld*GSK-3l isoform, and (vi) the need for total inhibition of the enzyme to get cellular effect (Knight and Shokat, 2005).

We next investigated the effects on cell-cycle progression and the death process induced by 5-Me-6-BIO treatment, using a number of different techniques. Its effect on parasite growth appeared to be more dose- than time-dependent, as the IC_{50} values did not significantly vary with the incubation time. However, 5-Me-6-BIO treatment affected the recovery potential of treated cells after removal of the drug, as cells were able to recover after 48 h of treatment, whereas 72 h of treatment caused an irreversible inhibition of cell growth.

In an effort to elucidate whether 5-Me-6-BIO targets *Ld*GSK-3s in vivo and the potential role of *Ld*GSK-3s in cell-cycle progression and apoptosis-like death a sat-*Ld*GSK-3s over-expressor mutant and a cell line expressing a kinase-dead mutant sat-*Ld*GSK-3s/K49R were generated. Cells that over-express *Ld*GSK-3s (about 2-fold) were about 2-fold less susceptible to growth inhibition than sat-*Ld*GSK-3s/K49R and sat transfectants at all time-points, indicating that the observed growth inhibition was closely associated with inhibition of *Ld*GSK-3s activity by 5-Me-6-BIO. In addition these results imply that the wild-type kinase should be inhibited by 5-Me-6-BIO with an IC_{50} value comparable with that of the His-tagged *Ld*GSK-3s. Also, the 2-fold increase in *Ld*GSK-3s expression in sat-*Ld*GSK-3s transfectants completely reversed the cell-cycle disruption effect of 5-Me-6-BIO and abolished the induction of apoptosis-like death. However, the *Ld*GSK-3s/K49R expression resulted in similar phenotypes with those of the sat transfectants. The results provide strong evidence that *Ld*GSK-3s is the intracellular target of 5-Me-6-BIO and suggest the direct or indirect involvement of *Ld*GSK-3s in cell-cycle control as well as in pathways leading to apoptosis-like death. Although there is evidence that apoptosis-like death occurs in *Leishmania* (Das et al., 2001) the pathways and proteins involved remain to be elucidated. GSK-3 is known to modulate apoptosis in mammalian cells by regulating the apoptotic pathways (Beurel and Jope, 2006). Therefore common pathways may exist between *Leishmania* and mammalian cells in regulating apoptotic signalling pathways through GSK-3.

In contrast to 5-Me-6-BIO, 6-BIO induced a time-dependent growth inhibition accompanied with a dose- and time-dependent accumulation of cells in G2/M. Moreover, 6-BIO induced apoptosis-like death in a lower proportion of promastigotes compared with 5-Me-6-BIO and this death process progressed more slowly in parasites exposed to 6-BIO. These differences between the cellular effects induced by 6-BIO compared with 5-Me-6-BIO suggest that in vivo the two indirubins may target different kinases and/or pathways.

The observation that over-expression of *Ld*GSK-3s only partially reversed the effect of 6-BIO is not unexpected, since in vitro 6-BIO preferentially inhibits CRK3. Moreover, the phenotype of promastigotes incubated with 6-BIO, especially the accumulation of cells in G2/M, is consistent with inhibition of CRK3, which is essential for cell-cycle progression at the G2/M phase transition (Grant et al., 1998; Hassan et al., 2001) and implies that CRK3 may be the main intracellular target of 6-BIO. Although 6-BIO was a more effective inhibitor of CRK3, and despite the observed phenotype being consistent with CRK3-inhibition, the fact that *Ld*GSK-3s over-expression partially reversed promastigote G2/M arrest and partially protected cells from 6-BIO induced apoptosis-like death, implies that 6-BIO may also target *Ld*GSK-3s in the parasite where the level of expression of the two kinases is not known. Since 6-BIO arrests promastigotes in G2/M phase of the cell-cycle, this may mean that *Ld*GSK-3s also plays a role in G2/M phase transition, although this is difficult to reconcile with the results for 5-Me-6-BIO. Alternatively, over-expression of *Ld*GSK-3s may influence 6-BIO activity by a non-specific mechanism (i.e. lower proportion of 6-BIO available for binding to and inactivating CRK3).

In conclusion, the complete reversal of the cellular effects induced by 5-Me-6-BIO in the over-expressing parasites strongly implies that *Ld*GSK-3s is the main target of 5-Me-6-BIO and suggests a potential role for *Ld*GSK-3s in cell-cycle progression and in apoptosis-like death. Moreover, the dramatic effect of *Ld*GSK-3s inhibitors on *Leishmania*, especially the intramacrophage amastigote stage, suggests that *Ld*GSK-3s has potential as a drug target in these parasites. Future work would be required to develop parasite-selective inhibitors that do not target host GSK-3 since its inhibition may affect the balance between Th1 and Th2 rsponses (Ohtani et al., 2008). In addition, RNA interference studies of *T. brucei* GSK-3 lead to similar cellular phenotypes, such as growth inhibition and altered parasite morphology (Ojo et al., 2008), to that caused by GSK-3 inhibitors in *Leishmania*. Importantly, the very recent validation of *Tbru*GSK-3 as a drug target for this protozoan parasite (Ojo et al., 2008), reinforces our claim that GSK-3 could constitute a trans-trypanosomatid as well as trans-protozoan target, including *P. falciparum* and that it should be exploited for anti-protozoan drug development.

Acknowledgements

This work was supported by HPI (E.X. PhD fellowship), by the General Secretariat of Research and Technology of Greece; PENED programme (V.M.), University of Athens programme Kapodistrias and by the FP6-2002-Life Sciences and Health, PRO-KINASE Research Project (L.M.). We thank our colleagues Dr. Christos Haralambous for the generation of the phylogenetic tree and Georgia Konidou for technical assistance.

Appendix A. Supplementary data

Supplementary data associated with this article can be found, in the online version, at doi:10.1016/j.ijpara.2009.04.005.

References

Alvar, J., Yactayo, S., Bern, C., 2006. Leishmaniasis and poverty. Trends Parasitol. 22, 552–557.

Barak, E., Amin-Spector, S., Gerliak, E., Goyard, S., Holland, N., Zilberstein, D., 2005. Differentiation of *Leishmania donovani* in host-free system: analysis of signal perception and response. Mol. Biochem. Parasitol. 141, 99–108.

Beurel, E., Jope, R.S., 2006. The paradoxical pro- and anti-apoptotic actions of GSK3 in the intrinsic and extrinsic apoptosis signaling pathways. Prog. Neurobiol. 79, 173–189.

Bohmer, F.D., Karagyozov, L., Uecker, A., Serve, H., Botzki, A., Mahboobi, S., Dove, S., 2003. A single amino acid exchange inverts susceptibility of related receptor tyrosine kinases for the ATP site inhibitor STI-571. J. Biol. Chem. 278, 5148–5155.

Chang, K.P., 1983. Cellular and molecular mechanisms of intracellular symbiosis in leishmaniasis. Int. Rev. Cytol. Suppl. 14, 267–305.

Croft, S.L., Sundar, S., Fairlamb, A.H., 2006. Drug resistance in leishmaniasis. Clin. Microbiol. Rev. 19, 111–126.

Damiens, E., Baratte, B., Marie, D., Eisenbrand, G., Meijer, L., 2001. Anti-mitotic properties of indirubin-3′-monoxime, a CDK/GSK-3 inhibitor: induction of endoreplication following prophase arrest. Oncogene 20, 3786–3797.

Das, M., Mukherjee, S.B., Shaha, C., 2001. Hydrogen peroxide induces apoptosis-like death in *Leishmania donovani* promastigotes. J. Cell Sci. 114, 2461–2469.

Davies, T.G., Tunnah, P., Meijer, L., Marko, D., Eisenbrand, G., Endicott, J.A., Noble, M.E., 2001. Inhibitor binding to active and inactive CDK2: the crystal structure of CDK2-cyclin A/indirubin-5-sulphonate. Structure 9, 389–397.

Doble, B.W., Woodgett, J.R., 2003. GSK-3: tricks of the trade for a multi-tasking kinase. J. Cell Sci. 116, 1175–1186.

Dujardin, J.C., 2006. Risk factors in the spread of leishmaniases: towards integrated monitoring? Trends Parasitol. 22, 4–6.

Frame, S., Cohen, P., Biondi, R.M., 2001. A common phosphate binding site explains the unique substrate specificity of GSK3 and its inactivation by phosphorylation. Mol. Cell 7, 1321–1327.

Grant, K.M., Hassan, P., Anderson, J.S., Mottram, J.C., 1998. The crk3 gene of *Leishmania mexicana* encodes a stage-regulated cdc2-related histone H1 kinase that associates with p12. J. Biol. Chem. 273, 10153–10159.

Grant, K.M., Dunion, M.H., Yardley, V., Skaltsounis, A.L., Marko, D., Eisenbrand, G., Croft, S.L., Meijer, L., Mottram, J.C., 2004. Inhibitors of *Leishmania mexicana* CRK3 cyclin-dependent kinase: chemical library screen and antileishmanial activity. Antimicrob. Agents Chemother. 48, 3033–3042.

Habtemariam, S., 2003. In vitro antileishmanial effects of antibacterial diterpenes from two Ethiopian *Premna* species: *P. schimperi* and *P. oligotricha*.. BMC Pharmacol. 3, 6.

Hanks, S.K., Quinn, A.M., 1991. Protein kinase catalytic domain sequence database: identification of conserved features of primary structure and classification of family members. Methods Enzymol. 200, 38–62.

Hassan, P., Fergusson, D., Grant, K.M., Mottram, J.C., 2001. The CRK3 protein kinase is essential for cell cycle progression of *Leishmania mexicana*. Mol. Biochem. Parasitol. 113, 189–198.

He, X., Saint-Jeannet, J.P., Woodgett, J.R., Varmus, H.E., Dawid, I.B., 1995. Glycogen synthase kinase-3 and dorsoventral patterning in *Xenopus* embryos. Nature 374, 617–622.

Hoessel, R., Leclerc, S., Endicott, J.A., Nobel, M.E., Lawrie, A., Tunnah, P., Leost, M., Damiens, E., Marie, D., Marko, D., Niederberger, E., Tang, W., Eisenbrand, G., Meijer, L., 1999. Indirubin, the active constituent of a Chinese antileukaemia medicine, inhibits cyclin-dependent kinases. Nat. Cell Biol. 1, 60–67.

Ilg, T., 2002. Generation of myo-inositol-auxotrophic *Leishmania mexicana* mutants by targeted replacement of the myo-inositol-1-phosphate synthase gene. Mol. Biochem. Parasitol. 120, 151–156.

Knight, Z.A., Shokat, K.M., 2005. Features of selective kinase inhibitors. Chem. Biol. 12, 621–637.

Laskowski, R., MacArthur, M., Moss, D., Thornton, J., 1991. PROCHECK: a programm to check the stereochemichal quality of protein structures. J. Appl. Crystallogr. 26, 283–291.

Meares, G.P., Jope, R.S., 2007. Resolution of the nuclear localization mechanism of glycogen synthase kinase-3: functional effects in apoptosis. J. Biol. Chem. 282, 16989–17001.

Meijer, L., Skaltsounis, A.L., Magiatis, P., Polychronopoulos, P., Knockaert, M., Leost, M., Ryan, X.P., Vonica, C.A., Brivanlou, A., Dajani, R., Crovace, C., Tarricone, C., Musacchio, A., Roe, S.M., Pearl, L., Greengard, P., 2003. GSK-3-selective inhibitors derived from Tyrian purple indirubins. Chem. Biol. 10, 1255–1266.

Meijer, L., Flajolet, M., Greengard, P., 2004. Pharmacological inhibitors of glycogen synthase kinase 3. Trends Pharmacol. Sci. 25, 471–480.

Mikus, J., Steverding, D., 2000. A simple colorimetric method to screen drug cytotoxicity against *Leishmania* using the dye Alamar Blue. Parasitol. Int. 48, 265–269.

Naula, C., Parsons, M., Mottram, J.C., 2005. Protein kinases as drug targets in trypanosomes and *Leishmania*. Biochim. Biophys. Acta 1754, 151–159.

Ohtani, M., Nagai, S., Kondo, S., Mizuno, S., Nakamura, K., Tanabe, M., Takeuchi, T., Matsuda, S., Koyasu, S., 2008. Mammalian target of rapamycin and glycogen synthase kinase 3 differentially regulate lipopolysaccharide-induced interleukin-12 production in dendritic cells. Blood 112, 635–643.

Ojo, K.K., Gillespie, J.R., Riechers, A.J., Napuli, A.J., Verlinde, C.L., Buckner, F.S., Gelb, M.H., Domostoj, M.M., Wells, S.J., Scheer, A., Wells, T.N., Van Voorhis, W.C., 2008. Glycogen Synthase Kinase 3 is a potential drug target for African trypanosomiasis therapy. Antimicrob. Agents Chemother. 52, 3710–3717.

Papageorgiou, F.T., Soteriadou, K.P., 2002. Expression of a novel *Leishmania* gene encoding a histone H1-like protein in *Leishmania major* modulates parasite infectivity in vitro. Infect. Immun. 70, 6976–6986.

Parsons, M., Worthey, E.A., Ward, P.N., Mottram, J.C., 2005. Comparative analysis of the kinomes of three pathogenic trypanosomatids: *Leishmania major*, *Trypanosoma brucei* and *Trypanosoma cruzi*. BMC Genomics 6, 127.

Polychronopoulos, P., Magiatis, P., Skaltsounis, A.L., Myrianthopoulos, V., Mikros, E., Tarricone, A., Musacchio, A., Roe, S.M., Pearl, L., Leost, M., Greengard, P., Meijer, L., 2004. Structural basis for the synthesis of indirubins as potent and selective inhibitors of glycogen synthase kinase-3 and cyclin-dependent kinases. J. Med. Chem. 47, 935–946.

Ribas, J., Garrofe-Ochoa, X., Boix, J., 2006. Characterization of the cell death processes triggered by indirubin derivatives in neuroblastoma cells. In: Meijer, L., Guyard, N., Skaltsounis, L.A., Eisenbrand, G. (Eds.), Indirubin, The Red Shade of Indigo, Life in Progress Editions, Roscoff, France, pp. 215–226.

Richard, O., Paquet, N., Haudecoeur, E., Charrier, B., 2005. Organization and expression of the GSK3/shaggy kinase gene family in the moss *Physcomitrella patens* suggest early gene multiplication in land plants and an ancestral response to osmotic stress. J. Mol. Evol. 61, 99–113.

Rosenzweig, D., Smith, D., Opperdoes, F., Stern, S., Olafson, R.W., Zilberstein, D., 2008. Retooling *Leishmania* metabolism: from sand fly gut to human macrophage. FASEB J. 22, 590–602.

Roy, G., Dumas, C., Sereno, D., Wu, Y., Singh, A.K., Tremblay, M.J., Ouellette, M., Olivier, M., Papadopoulou, B., 2000. Episomal and stable expression of the luciferase reporter gene for quantifying *Leishmania* spp. infections in macrophages and in animal models. Mol. Biochem. Parasitol. 110, 195–206.

Sali, A., Blundell, T.L., 1993. Comparative protein modelling by satisfaction of spatial restraints. J. Mol. Biol. 234, 779–815.

Smirlis, D., Bisti, S.N., Xingi, E., Konidou, G., Thiakaki, M., Soteriadou, K.P., 2006. *Leishmania* histone H1 overexpression delays parasite cell-cycle progression, parasite differentiation and reduces *Leishmania* infectivity in vivo. Mol. Microbiol. 60, 1457–1473.

Stewart, J.J., 1990. MOPAC: a semiempirical molecular orbital program. J. Comput. Aided Mol. Des. 4, 1–105.

Wells, C., McNae, I., Walkinshaw, M., Westwood, N.J., Grant, K.M., 2006. The selective biological activity of indirubin-based inhibitors: applications in parasitology. In: Meijer, L., Guyard, N., Skaltsounis, L. A., Eisenbrand, G (Eds.), Indirubin, The Red Shade of Indigo, Life in Progress Editions, Roscoff, France, pp. 259–267.

Wiesgigl, M., Clos, J., 2001. Heat shock protein 90 homeostasis controls stage differentiation in *Leishmania donovani*. Mol. Biol. Cell 12, 3307–3316.